

Heat production in granitic rocks: Global analysis based on a new data compilation GRANITE2017



Irina M. Artemieva^{a,b,*}, Hans Thybo^{b,c}, Kiki Jakobsen^a, Nanna K. Sørensen^a, Louise S.K. Nielsen^a

^a IGN, University of Copenhagen, Øster Voldgade 10, Copenhagen 1350, Denmark

^b Eurasia Institute of Earth Sciences, Istanbul Technical University, Istanbul 34469, Turkey

^c Centre for Earth Evolution and Dynamics (CEED), University of Oslo, Oslo N-0315, Norway

ARTICLE INFO

Keywords:

Heat production
Th/U ratio
K/U ratio
Supercontinents
Urey ratio
Continental crust

ABSTRACT

Granitic rocks play special role in the dynamics and evolution of the Earth and its thermal regime. First, their compositional variability, reflected in the distribution of concentrations of radiogenic elements, provides constraints on global differentiation processes and large scale planetary evolution, where emplacement of granites is considered a particularly important process for the formation of continental crust. Second, heat production by radioactive decay is among the main heat sources in the Earth. Therefore knowledge of heat production in granitic rocks is pivotal for thermal modelling of the continental lithosphere, given that most radiogenic elements are concentrated in granitic rocks of the upper continental crust whereas heat production in rocks of the lower crust and lithospheric mantle is negligible.

We present and analyze a new global database GRANITE2017 (with about 500 entries) on the abundances of heat producing elements (Th, U, K) and heat production in granitic rocks based on all available published data. Statistical analysis of the data shows a huge scatter in all parameters, but the following conclusions can be made. (i) Bulk heat production in granitic rocks of all ages is ca. $2.0 \mu\text{W}/\text{m}^3$. It is very low in Archean-Early Proterozoic granitic rocks (1.67 ± 1.49 and $1.25 \pm 0.83 \mu\text{W}/\text{m}^3$, respectively) and there is a remarkable peak in heat production in Middle Proterozoic granites (presently $4.36 \pm 2.17 \mu\text{W}/\text{m}^3$) followed by a gradual decrease towards Cenozoic granites ($3.09 \pm 1.62 \mu\text{W}/\text{m}^3$). Low heat production in the ancient continental crust may be important for preservation of cratonic lithosphere. (ii) There is no systematic correlation between the tectonically controlled granite-type and bulk heat production, although A-type (anorogenic) granites are the most radioactive, and many of them were emplaced in Middle Proterozoic. (iii) There is no systematic correlation between heat flow and concentrations of radiogenic elements. (iv) The present-day global average Th/U value is 4.75 ± 4.27 with a maximum in Archean-Early Proterozoic granites (5.75 ± 5.96) and a minimum in Middle-Late Proterozoic granites (3.78 ± 2.69). The Th/U ratio at the time of granite emplacement has a minimum in Archean (2.78). (v) The present-day K/U ratio is close to a global estimate for the continental crust only for the entire dataset ($1.46 \pm 1.63 \times 10^4$), but differs from the global ratio for each geological time, and all anomalously high values are observed only in Archean-Early Proterozoic granites. (vi) We do not observe a systematic difference in radiogenic heat production between Archean and post-Archean granites, but rather recognize a sharp change in radiogenic concentrations and ratios from the Early Proterozoic to Middle Proterozoic granites. The Proterozoic anomaly may be caused by major plate reorganizations possibly related to the supercontinent cycle when changes in the granite forming processes may be expected, or it may even indicate a change in global thermal regime, mantle dynamics and plate tectonics styles. (vii) Our results provide strong evidence that secular change in the Urey ratio was not monotonous, and that plate motions may have been the fastest in Middle Proterozoic and have been decreasing since then. (viii) We estimate the total present-day heat production in the granitic crust as 5.8–6.8 TW and in the continental crust as 7.8–8.8 TW.

1. Introduction

Continental crust is formed under different conditions than oceanic.

The exact processes and their relative roles are still debated even for modern environments (Kemp and Hawkesworth, 2003; Rudnick and Gao, 2003). Several lines of evidence suggest that formation of the

* Corresponding author at: IGN, University of Copenhagen, Øster Voldgade 10, Copenhagen 1350, Denmark.
E-mail address: irina@ign.ku.dk (I.M. Artemieva).

continental crust is a multi-stage process, which includes at the first stage production of basaltic magmas by mantle melting followed by later re-melting, fractional crystallization, and differentiation to produce the continental crust with a bulk andesitic composition (Kelemen, 1995; Rudnick, 1995).

The mechanisms of formation of the ancient continental crust are subject to rigorous debates (Amelin et al., 1999; Hawkesworth and Kemp, 2006; Hamilton, 2013). It is also unknown when the first continental crust was formed (Harrison et al., 2005; Reimink et al., 2016), how much may have been preserved, and how fast it may have been recycled into the mantle (Hawkesworth et al., 2009; Condie, 2014). As a consequence of the poor understanding of the evolution of the continental crust there is an enormous diversity in models of secular crustal growth, which range from Armstrong's model of a nearly instantaneous crustal growth in the Hadean (Armstrong, 1981), to models of episodic crustal growth (Condie, 1998), and numerous models which favor gradual crustal growth since the Archean (e.g. Belousova et al., 2010). Therefore, information on systematic variations of the composition of the continental crust, and in particular the upper crust, provides crucial insight into the geodynamic conditions on early Earth (Taylor and McLennan, 1985, 1995).

Continental crust consists on average of ca. 61% of SiO₂ and is compositionally stratified. The principal characteristics of continental crust, in comparison to oceanic crust, is the presence of an upper layer of felsic composition. Borehole data, geological studies of basement outcrops, and high-resolution seismic studies complemented by laboratory measurements of seismic velocities in different rocks types, all indicate that granitic rocks dominate the composition of the upper continental crust. The thickness of the granitic upper crust is commonly 10–20 km (Christensen and Mooney, 1995; Artemieva and Thybo, 2013; Cherepanova et al., 2013) and therefore its contribution to surface heat flow through radioactive decay is significant, 10–20 mW/m² for bulk radiogenic heat production of 1.0 μW/m³, which makes up to 50% of a typical surface heat flow in stable continents.

Granitic rocks are unique among common rock types in having high concentrations of heat producing radioactive elements, namely U, Th, and K (Jaupart and Mareschal, 2003). Transport of materials rich in heat-producing and other large-ion lithophile (LIL) elements to the middle and upper crustal levels may take place through various processes associated with high-grade metamorphism, metasomatism, partial melting, and fluid and melt migration (Taylor and McLennan, 1985). Potassium is one of the LIL elements and it tends to concentrate in granites as an essential element of such common rock-forming minerals as phlogopite, muscovite and biotite. Its concentration in granitic rocks increases with the silica content (Fig. 1). Thorium and uranium are also LIL elements, but because of lower overall abundances they are present mostly in trace minerals in common rocks (Van Schmus, 1995) and show poor correlation with the silica content (Fig. 1).

On the whole, the chemical behavior of U, Th, K is dissimilar, but all three being LIL elements, they exhibit similar tendencies in large-scale processes. Geochemical and cosmo-chemical models predict the following global mean ratios of occurrence

$$K/U = (1.0\text{--}1.3) \times 10^4 \text{ and } Th/U = (3.7\text{--}4.0)$$

for the bulk Earth and primitive mantle (Taylor and McLennan, 1985) with a significant variability reported for continental crust (Wedepohl, 1995; McLennan, 2001; Rudnick and Gao, 2003; Arevalo et al., 2009; Hacker et al., 2011; Table 1). At the same time, regional processes, such as weathering, e.g. associated with migration of hydrous solutions, may lead to selective leaching of one or more of the heat producing isotopes, in particular uranium, which is the most soluble of the heat producing elements at low temperatures (Buntebarth, 1976).

In geophysical studies, heat production in rocks is a key parameter for geothermal modeling (Rudnick et al., 1998; Artemieva and Mooney, 2001; Jaupart and Mareschal, 2003). However, it is also the least known parameter because heat production does not correlate with

macroscopic properties of rocks (e.g. Vp, Vs, density, etc.) (Rybäck and Buntebarth, 1982; Fountain, 1985; Kukkonen and Peltoniemi, 1998), in particular since Th and U are hosted chiefly by accessory phases and thus cannot have any strong effect on seismic velocities and density. However, heat production is, to some degree, correlated with SiO₂ content (c.f. Artemieva, 2011) (Fig. 2).

Importantly, due to radioactive decay, heat production decreases with age, and in a different way for different rock types, because the major radioactive isotopes in crustal rocks, U, Th, and K, have different concentrations, different decay constants and different abundances (van Schmus, 1995; Jaupart and Mareschal, 2003) (Table 2). For example, the relative contribution of ²³²Th to heat production increases with time because this element has the longest half-life of the three isotopes, while the contribution of ²³⁵U was dominant largely on early Earth and has been fast decreasing during planetary evolution (Table 3, Fig. 3). Isotopic abundances are also highly variable. For example, radioactive ⁴⁰K makes only a tiny fraction of potassium isotopes, which are dominated by nonradioactive ³⁹K (ca. 93%) and ⁴¹K (ca. 7%). On the whole, available data indicate that (except for low-radiogenic oceanic arc granites) post-Archean rocks have higher concentration of heat producing elements than Archean rocks (Fig. S1).

Variations in heat production on a regional scale have been the focus of numerous studies on different continents (Ashwal et al., 1987; Jones, 1987; Pinet and Jaupart, 1987; Inger and Harris, 1993; Guillou-Frottier et al., 1995; Furukawa and Shinjoe, 1997; Kukkonen and Peltoniemi, 1998; Roy and Rao, 2000; Kemp, 2001). They provide important information on variations in radioactive elements in different continental settings and usually link regional differences in heat production to variations in lithology and metamorphic grade. With few exceptions, variations within the same rock type (e.g. in granites) can hardly be analyzed in a statistically representative fashion due to a small number of rock samples used in regional studies. A systematic analysis of heat production data for different common lithologies based on extensive data sets has been undertaken in some studies (Wollenberg and Smith, 1987; Vila et al., 2010), but without link to tectonic setting, which is particularly important for granitic rocks, where their tectonic origin may significantly control their chemical characteristics (Kemp and Hawkesworth, 2003) and therefore concentration of radioactive elements (Kemp, 2001).

A systematic analysis of heat production in granites is of particular importance for both models of crustal evolution and thermal modeling, because the granitic upper crust provides the highest contribution to surface heat flow (heat generated by radiogenic decay of the isotopes ²³²Th, ²³⁵U, ²³⁸U, and ⁴⁰K). This contribution regionally varies from ca. 30% to 80–90% (Artemieva and Mooney, 2001) with the highest contribution in granitic plutons. A systematic analysis has, so far, never been performed globally due to the absence of a representative database, while numerous regional studies provide valuable information on significant variations of heat production in granitic rocks even within the same geological provinces (c.f. Kemp and Hawkesworth, 2003). Dedicated analyses have been carried out for A-type (anorogenic) granites (Whalen, 1985) and I- and S-type granites (see Table 4 for details) of the Lachlan Fold Belt (Chappell and White, 1992), but similar global studies are absent for different granite types and for granitic rocks in general. Regional data, however, clearly demonstrate a huge variability in the concentrations of U, Th, and K in different types of granites (Fig. 1, Fig. S1).

The goal of our study is to examine heat production in granites worldwide through statistical analysis of a globally representative dataset on concentrations of heat producing radioactive elements (U, Th, and K) and heat production in granitic rocks from different continental settings. Our interest is on a global scale rather than to focus on a particular region, in order to examine large-scale patterns and possible trends in global variations in the occurrence of radiogenic elements and heat production in granites. The open-access database of the International Heat Flow Commission (IHFC) focuses chiefly on heat

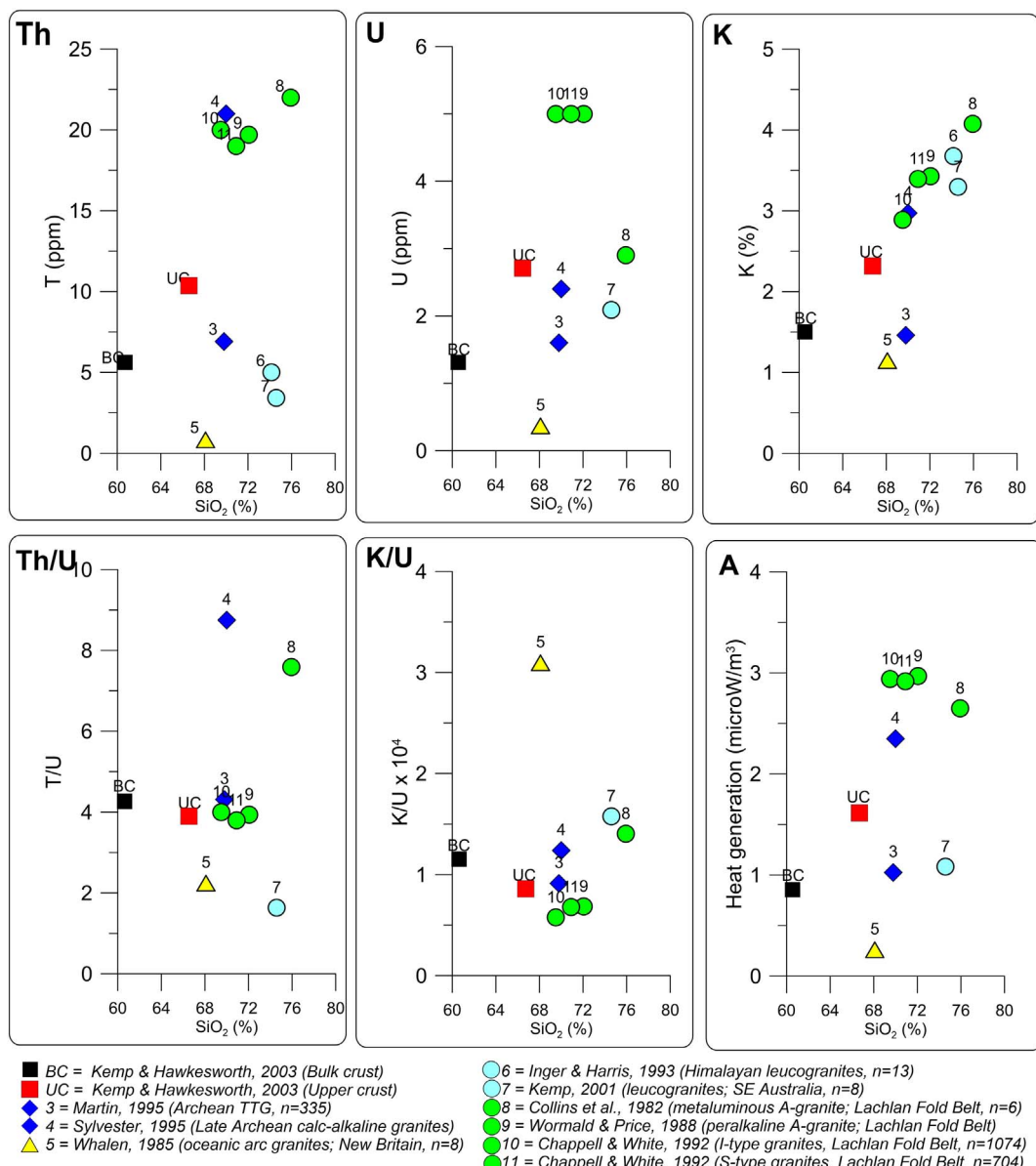


Fig. 1. Concentrations of Th, U, K, the ratios of Th/U and K/U, and bulk heat production in granitic rocks of different ages and from different settings. In general, there is no correlation between the silica content and the concentrations of Th and U, while K concentration shows some correlation with the SiO₂ content. Oceanic arc granites (yellow symbols) are low-radioactive.

Table 1
Abundances of K, U, Th in continental crust.^a

	Th, ppm	U, ppm	K, %	Th/U	K/U ($\times 10^4$)
USGS granite G-1	50	3.4	4.45	14.71	1.31
USGS granite G-2	24	3.0	3.67	8.0	1.22
Average upper cont. crust	10.5	2.5	2.7	4.2	1.08
Average post-Ar cont. crust	4.8	1.25	1.27	3.84	1.02
Average Archean cont. crust	3.5	0.91	0.91	3.85	1.00

^a Data from Van Schmus (1995).

flow data and, although it includes some information on heat production (where measured and reported), this type of data is incomplete and in most instances missing in the database. Further, data on heat production are not included to the IHFC database when heat flow values have not been reported. The general absence of information on rock composition also makes the IHFC database unsuitable for a targeted analysis of heat production in granites. We therefore have compiled a

global database of heat production in granitic rocks GRANITE2017 (Supplementary Data), which we use here for our analysis.

2. Classification of granitic rocks

Granites, together with tonalites, granodiorites, diorites, and quartz monzonites, are plutonic rocks rich in quartz and plagioclase, and are generally termed as granitoid rocks (Fig. 4). Based on geodynamic origin and geochemical characteristics, granitic rocks are commonly subdivided into the A-, I-, S-, and M-types (Table 4), although this alphabetical (S-I-A-M) classification of granitic rocks has been criticized (Frost et al., 2001; Bonin, 2007). Other types (H- and C-) have been also proposed but these classes are not used widely.

The alphabetical classification began with geochemical studies of granites from the Lachlan Fold Belt in southeastern Australia, which led to the conclusion that they generally fall into two groups with distinct compositions which reflect the composition of their source rock (Chappell and White, 1974, 2001). Hornblende-bearing I-type granites in the eastern part of the Lachlan Fold Belt were proposed to be formed

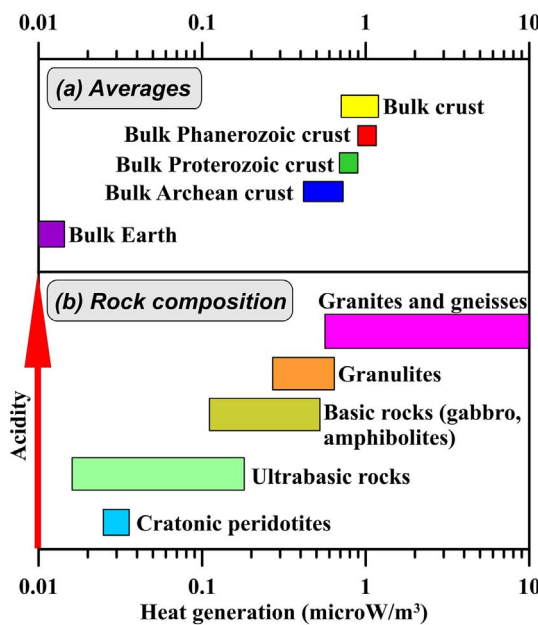


Fig. 2. Heat production for different rocks. (a) Average values for the bulk continental crust and the bulk Earth; (b) General trends in heat production variations in common crustal and upper mantle rocks (modified after Artemieva, 2011 based on data of Nicolaysen et al., 1981; Weaver and Tarney, 1984; Taylor and McLennan, 1985; Fountain, 1986; Shaw et al., 1986; Ashwal et al., 1987; Fountain et al., 1987; Pinet and Jaupart, 1987; Rudnick and Presper, 1990; Ketcham, 1996; McLennan and Taylor, 1996; Gao et al., 1998; Rudnick et al., 1998; Rudnick and Nyblade, 1999; Beardmore and Cull, 2001).

Table 2
Heat producing radioactive elements in the upper crust.^a

Isotope	Half-life (Gy)	Specific isotopic heat production ($\mu\text{W/kg}$)	Isotope abundances at present (wt%)	Isotope abundance assuming it equals 1.0 at present	
				1.0 Gy ago	4.5 Gy ago
⁴⁰ K	1.3	29	0.0119	1.7	10.9
²³² Th	13.9	26	100	1.05	1.25
²³⁵ U	0.7	569	0.7110	2.64	80
²³⁸ U	4.5	94.7	99.2834	1.17	2.0

^a Based on van Schmus (1995).

Table 3
Secular variations in relative radioactive heat production in the bulk Earth.^a

Time before present	Geological period	Radioactive heat production (as fraction of the total at present)			
		Due to K	Due to Th	Due to U	Total
0 Gy	Now	0.15	0.42	0.43	1.00
0–0.5 Gy	Phanerozoic	0.18	0.43	0.45	1.06
0.5–2.0 Gy	Late-Mid Proterozoic	0.33	0.46	0.57	1.36
2.0–3.5 Gy	Early Proterozoic – Archean	0.75	0.49	0.97	2.21

^a Based on van Schmus (1995).

by partial melting of igneous source rocks that have not undergone surface weathering, whereas the origin of the cordierite-rich S-type granites, which dominate the western part of the Lachlan Fold Belt, was attributed to partial melting of metasedimentary rocks.

The A-type granites (Loiselle and Wones, 1979) are typical of intraplate, anorogenic settings, and most of them were emplaced in the

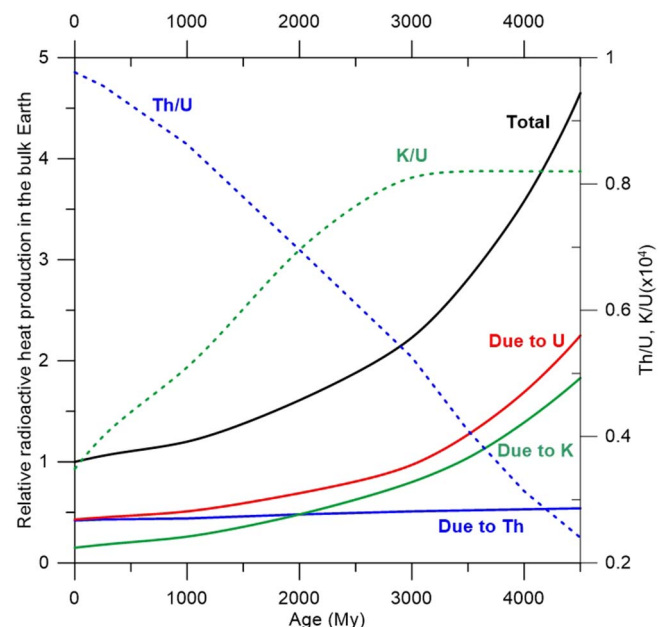


Fig. 3. Relative radioactive heat production in the bulk Earth normalized by its present-day value (see Table 3 for details, based on data of van Schmus, 1995).

Proterozoic (at ca. 1.8–1.5 Ga), such as the rapakivi-type (which are technically I-type) granites in southern Finland and Greenland, and the vast anorogenic granitic belts of the Adirondack mountains (eastern Canada) and south-eastern Australia. These granites usually have high silica content and are potassium-rich.

The major problem with the alphabetical classification is that it assumes a simple source for individual granitic rocks, which is rarely the case. In most cases, granites are formed as mantle-derived melts contaminated by crustal melting. Another problem is that while the definition of I- and S-types strictly was based on the inferred difference in the sources of the granites (Chappell and White, 1974), the identification of A-type granitoids includes both tectonic setting and chemical characteristics (Loiselle and Wones, 1979). We, nonetheless, use the alphabetical classification to discuss heat production in granitic rocks, given that different types of granitic rocks are, in general, characteristic of different tectonic settings (Table 4).

3. Database GRANITE2017 of heat production and K, U, Th concentrations in granitic rocks

3.1. Database structure and coverage

The granitic database GRANITE2017 is constrained by compilation of data from original publications where information on rock type, heat production, and concentration of radiogenic elements has been reported (Table 5). Where possible, information on tectonic setting, the terrane age and the age of the granitic rocks emplacement was included as well. Since our interest is solely in granitic rocks, oceanic regions have been excluded from the compilation. Our original ambition was to examine global patterns of heat production associated with different types of granites (A-, I-, and S-types); but we found this impossible, because information on granite types is commonly absent in the geochemical literature, while geochemical reviews commonly report regionally averaged values for radiogenic heat production.

We recognize that our compilation is limited geographically (Fig. 5), with a strong bias towards data from a limited number of tectonic provinces (Table 5). This is due to the limited availability of the required data, and we would be happy to extend the database with data from other regions, when the necessary information may become publicly available through international publications. Nonetheless,

Table 4
Tectonic settings of different granite types.

Granite type	Source	Composition	Tectonic setting	Examples	Key references
S-type	Partial melting of metasedimentary source rocks in collisional zones	Peraluminous granitoid rocks; high SiO_2 (65–79%); high K/Na ratio; key modal minerals: muscovite, biotite, ilmenite and garnet; common range of rock types:	Syn-collisional granitoids from intracontinental collisional zones and the cores of overthickened metamorphic belts	Archean: Western Superior (Canadian Shield); Proterozoic: the Tasman Mobile Belt (Eastern Australia); Meso-Cenozoic: Himalayas	Chappell and White, 1974, 2001; Clemens and Wall, 1981
I-type	Partial melting of predominantly igneous protolith, intermediate to mafic source material, melting of lower continental crust	Leucogranite to granodiorite Metalluminous granites, peralkaline granitoid rocks; SiO_2 53–76 wt%; low K/Na ratio; key modal minerals: hornblende, biotite and pyroxene; common range of rock types: granite to gabbro	Continental volcanic arcs	Archean: TTG gneisses; Proterozoic: the Tasman Mobile Belt (Eastern Australia). Paleozoic: Lachlan Fold Belt (Eastern Australia) Mesozoic: Cordilleran batholiths of W. USA and NW Mexico	Chappell and White, 1974, 2001
A-type	A1 - OIB-like mantle source, variably contaminated by crustal material. A2 - differentiation of a continental tholeiite, with variable degrees of crustal interaction. The origin of all A-granites cannot be explained by one petrogenetic model.	Peraluminous to peralkaline granitoid rocks; high SiO_2 (ca. 60–80%), iron-rich; include syenites and rhyolites; common range of rock types: alkali granite to anorthosite gneiss	Post-orogenic (anorogenic and/or anhydrous) granitoids, within the extensional tectonic environment (continental rifts) and within stable continental (cratonic) interior (hot spots)	Late Archean: Keivy anorthosite complex (NE Baltic Shield); Ylgarn (W. Australia), Abitibi (Superior province), S. Greenland; Proterozoic: rapakivi granites (S. Baltic shield); Bushveld complex (S. Africa); Seychelles archipelago; Paleozoic: the White Mountain igneous province (NE USA), Hoggar and Air domes (Sahara); W. Argentina, Caledonian granitoids of Ireland and Britain; Oslo rift. Meso-Cenozoic: S. end of the East African Rift (Malawi); afar (Ethiopia); S. China; Snake River Plain (USA); SE Iceland Similar to Archean TTG and adakites	Loiselle and Wones, 1979; Eby, 1992, 2011; Bonin, 2007
M-type (rare)	Melting of subducted oceanic crust (technically, I-type granites) or direct mantle melting	SiO_2 46–73 wt%; low K/Na ratio; key modal minerals: hornblende, clinopyroxene, biotite; common range of rock types: quartz diorite to gabbro	Oceanic island arcs, subduction zones	White, 1979	

Composition of an average granite

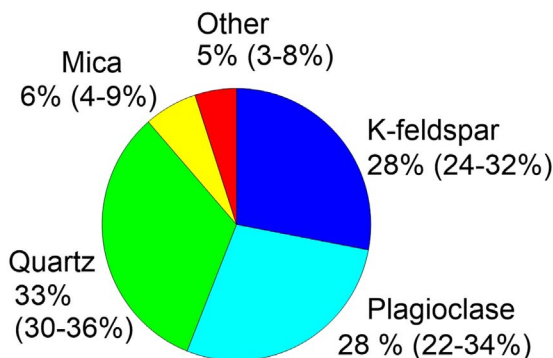


Fig. 4. Composition of an average granite.

Table 5

Statistics for the GRANITE2017 database on heat production in granites.

	Number of data points ^a			
	Heat production	U	Th	K
Africa	61	52	52	52
Australia	22	5	5	3
Canada	68	62	62	62
USA	94	54	54	54
China	120	103	103	2
India	11	10	10	10
Europe	108	21	21	21
Total	484	307	307	204
Uncertainty of individual entries	2–10%	ca. 3%	ca. 3%	ca. 3%

^a Note: importantly, many entries are averages for several boreholes with heat flow measurements, so that the true number of measurements is significantly larger than the number of entries in the database.

the database provides a statistically representative sampling of granitic rocks from different continental settings, but its geographical limitations should be kept in mind in discussion of the results of our analysis.

Large uncertainty in the database is associated with the age of granites, and in most cases age information is not available in the original publications which report data on heat production. Therefore, our analyses of secular trends is based on the age of crustal terranes, which in some cases (e.g. the Rio Grande Rift zone) provides older ages than the emplacement age of the granitic rocks. The analysis is presented for

Table 6
Age groups used in the database.

Group	Age range (Ma)	Geological epoch	Number of data for age of granites	Number of data for age of crustal province
1	0–250	Meso-Cenozoic	167	88
2	250–542	Paleozoic	88	50
3	542–1000	Late Proterozoic	32	67
4	1000–1800	Middle Proterozoic	26	24
5	1800–2500	Early Proterozoic	48	127
6	2500–3800	Archean	98	107

Note: the same age subdivision is used for the age of the crustal provinces and for the emplacement age of granitic rocks.

six age groups (Table 6).

3.2. Uncertainties of individual entries

Heat production values, A, are computed from known (measured) concentrations of U, K and Th (C_U , C_K and C_{Th}) based on the relationship originally proposed by Birch (1954) and slightly modified later (Rybáček, 1988):

$$A(\mu\text{W/m}^3) = \rho(0.0952 C_U + 0.0348 C_K + 0.0256 C_{Th}) \quad (1)$$

where ρ is density in g/cm^3 , and C_U , C_K and C_{Th} are concentrations of radioactive isotopes in ppm, % and ppm, respectively. ^{40}K concentration is commonly reported as K_2O (Table 2). For consistency, we converted K_2O values (molar mass ca. $39 \times 2 + 16 = 94$) to K concentrations by multiplying the K_2O values by 0.83 ($= 78/94$). Commonly, an average density of 2.70 g/cm^3 is used to calculate heat production for all lithologies, and we used the same value of density to calculate the heat production in granitic rocks when this value was not reported in original publications. A change of the assumed density value from 2.70 to 2.65 g/cm^3 will produce an uncertainty in heat production of ca. 2%.

Uncertainties in concentrations of U, K and Th also contribute to the overall uncertainty in heat production. Regional study in the Canadian Shield (Ashwal et al., 1987) estimated the average standard deviations of individual heat production determinations for different lithologies as $0.06 \mu\text{W/m}^3$, with a range from 0.05 to $0.18 \mu\text{W/m}^3$ for granitic rocks. It gives an uncertainty of ca. 2–10% for the heat production value (Ashwal et al., 1987), which we estimate to be a representative

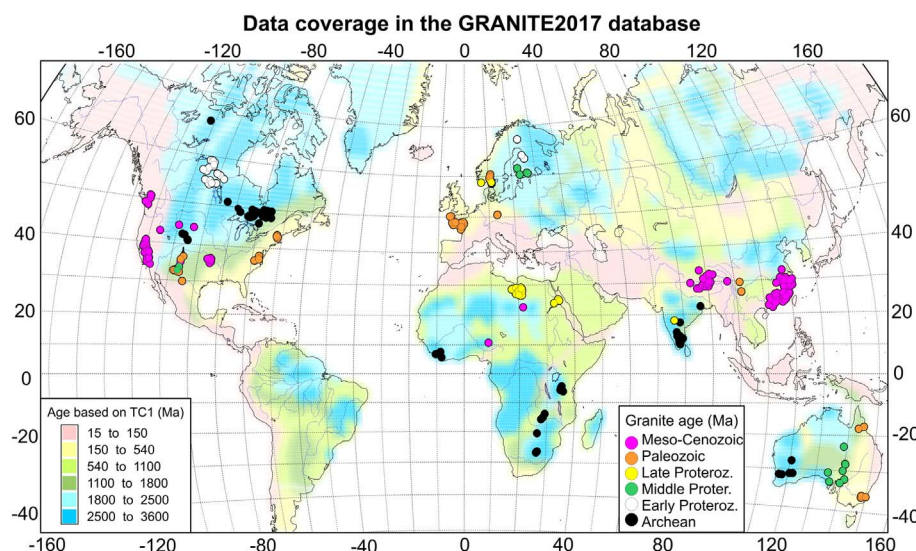


Fig. 5. Data coverage in the granite database GRANITE2017. Background – age of crustal provinces based on the TC1 model (Artemieva, 2006), dots – locations of granites included to the database, colors refer to the emplacement ages.

Table 7
Present-day heat production in silicate Earth.

	Th, ppm	U, ppm	K, %	Total heat production, TW	Uncertainty	Reference
Granitic rocks (GRANITE2017, all data)	14.8 ± 13.2	3.93 ± 3.27	2.79 ± 1.44	5.8–6.8 ^{a,b}	~70%	Present study
Continental crust	–	–	–	7.8–8.8 ^c	~70%	Present study
Continental crust	5.6	1.3	1.5	7.5 ± 2.5 ^e	> 30%	Rudnick and Gao, 2003
Depleted mantle ^d	13.7 ± 4.1	4.7 ± 1.4	60 ± 17	4.2 ± 1.4	30%	Salters and Stracke, 2004
Depleted mantle	16	8	100	5.5 ^f	?	Jochum et al., 1983
Depleted mantle	–	–	–	8.5 ± 5.5	65%	Korenaga, 2008
BSE	80	20	240	20	?	McDonough and Sun, 1995
BSE	63 ± 11	17 ± 3	190 ± 40	16 ± 3	20%	Lyubetskaya and Korenaga, 2007
Mantle				10–30		The KamLand Collaboration, 2011

^a Based on averages for compiled heat production values and calculated based on average concentrations of heat producing elements (Table 12).

^b Assuming granitic rocks make 1/3 of the volume of continental crust of $7.6 \times 10^9 \text{ km}^3$ (Taylor and McLennan, 1995).

^c Based on heat production in granitic rocks^b and assuming that non-granitic (intermediate and mafic) crust with average heat production of $0.4 \mu\text{W/m}^3$ (Rudnick and Fountain, 1995) makes 2/3 of the volume of continental crust.

^d Depleted mantle (DM) makes 82% of mantle mass with the remaining 18% making the enriched mantle (EM) reservoir at the base of the mantle (Arevalo et al., 2013).

^e Assuming the mass of continental crust of $2.3 \times 10^{22} \text{ kg}$.

^f Calculated based on Eq. (1) assuming mantle density of 3.4 t/m^3 .

uncertainty value for the entire database.

4. Global thermal budget

We use the GRANITE2017 database to calculate average heat production and concentrations of heat producing elements in granitic rocks (Table 7). The continental crust, through radioactive decay of heat producing elements, contributes about 1/3 of the total radiogenic heat loss of the Earth (Huang et al., 2013). Heat producing elements responsible for radiogenic heat are concentrated mostly in the bulk silicate Earth, which includes depleted and enriched reservoirs within the convective mantle, lithospheric mantle, continental and oceanic crust. Geochemical models of composition of the bulk silicate Earth (Table 7) yield ca. 20 TW for its present-day internal heat production (McDonough and Sun, 1995; Allegre et al., 2001), although the value is still debated.

An alternative way of assessing radiogenic decay processes in Earth's interior and thus of estimating the global thermal budget is based on detection of antineutrinos that are emitted during radioactive decay of heat producing elements in the crust, the upper mantle, and the lower mantle (Table 8) (Eder, 1966; Krauss et al., 1984; Kobayashi and Fukao, 1991). However, due to the low energy released by the ^{40}K decay (Table 8), antineutrinos produced by this decay are difficult to resolve (Korenaga, 2008). By detecting antineutrinos emitted by radiogenic decay in different layers within Earth's interior and assuming that they are distributed spherically symmetric, one may constrain the average heat production in each of these layers (Mantovani et al., 2004). However, the resolution of this method decreases with the source depth and thus the method provides the best constraints for the upper layers (the crust).

Since the first results obtained by the Kamioka liquid scintillator antineutrino detector (KamLAND) (Araki et al., 2005; McDonough, 2005), the geoneutrino method has been rapidly developing over the

past decade. The estimates of the global thermal budget by the geoneutrino method still provide results with a large uncertainty, and the estimate of the flux from the mantle is 10–30 TW (The KamLand Collaboration, 2011), which is in general agreement with global constraints based on mantle composition. The total global surface heat flux is estimated to be around 44–46 TW (Pollack et al., 1993; Jaupart et al., 2007), with the difference between the internal heat production and surface heat flux being due to secular cooling, including energy release from solidification at the top of the inner core, and energy release by plate tectonic and mantle dynamic processes. These estimates assume a total heat production in the continental crust of 7.5 TW (Rudnick and Gao, 2003).

The upper continental crust plays a major role in the global thermal budget, since most of heat producing elements are concentrated in granitic rocks (Fig. 2). A recent assessment of heat generation in the crustal layers based on geoneutrino data (Huang et al., 2013) places the abundances of Th, U, and K in the upper continental crust at $10.5 \pm 1.0 \text{ ppm}$, $2.7 \pm 0.6 \text{ ppm}$ and $2.3 \pm 0.2\%$, respectively. These values were used as the basis for a recent global reference model for the abundances and distributions of heat producing elements in the crust (Usman et al., 2015). However, our results suggest significantly higher concentrations of heat producing elements in the upper, granitic, crust: 14.8 ppm, 3.93 ppm, and 2.79%, for Th, U, and K respectively (Table 7).

Assuming that granitic rocks make 1/3 of the volume of continental crust, i.e. assuming that a typical continental crust has a ca. 13–15 km thick upper crustal layer (e.g. Artemieva and Thybo, 2013; Cherepanova et al., 2013; Xia et al., 2017), our results (Table 7) suggest that the total heat production in the continental crust is slightly higher than commonly assumed, ca. 7.8–8.8 TW. It implies that the total surface heat flow may be also higher than commonly accepted, up to ca. 47–48 TW.

5. Secular changes in heat production and the supercontinent cycle

5.1. General patterns

We focus our analysis on the following:

- global patterns of distribution of heat production (A) and concentrations of uranium (U), thorium (Th) and potassium (K) in granitic rocks worldwide as well as their statistical analysis;
- global correlations between A, U, Th, K and surface heat flow, which we also examine as a function of crustal age, the age of granite emplacement, composition of the granitic rocks, and the S-I-A-M-

Table 8

Energy associated with radioactive decay of heat producing elements.^a

Parent isotope	Daughter isotope	Emitted electrons, number	Emitted neutrino, number	Emitted antineutrino, number	Released energy, MeV
238U	206Pb	6	0	6	51.7
235U	207Pb	4	0	4	46.0
232Th	208Pb	4	0	4	42.7
40K (89.3%)	40Ca	1	0	1	1.31
40K (10.7%)	40Ar	– 1 ^b	1	0	1.51

^a Based on Korenaga (2008).

^b Electron capture.

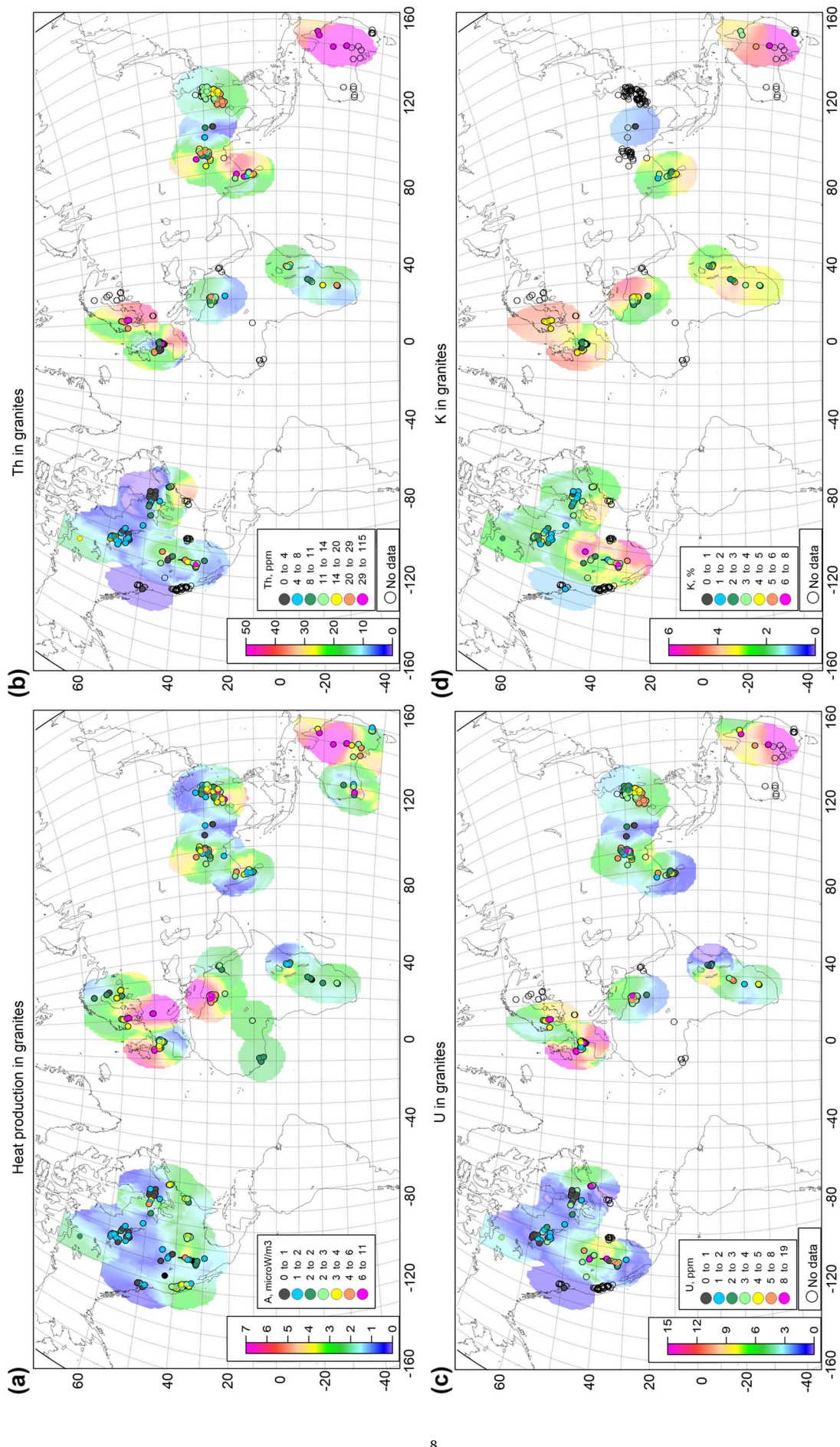


Fig. 6. Heat production in granitic rocks and concentrations of Th, U, K based on the granite database GRANITE2017 (dots – point data; background colors – interpolation with the same units as for point data).

- granite type;
- distribution of Th/U and K/U ratios in granitic rocks of different ages worldwide.

We analyze separately (Section 7.2) heat production and concentrations of heat producing elements at the time of granite emplacement and discuss the implications of these secular variations for Precambrian plate tectonics and mantle dynamics. We emphasize that our compilation has significant limitations due to the uneven data coverage, with overrepresentation of some regions (China) and underrepresentation of other regions (Table 5, Fig. 5). These limitations should be kept in mind, in particular for interpretations of the statistical analysis of data. However, we consider that the database allows us to recognize the first-order global patterns.

We observe significant variability in concentrations of uranium, thorium and potassium in granitic rocks worldwide (Fig. 6). In broad terms, the lowest concentrations of Th and U, and therefore, low heat production values ($< 1\text{--}2 \mu\text{W/m}^3$) are typical of granites of the Canadian shield, Tanzanian craton and the magmatic arc of western Canada, while moderate values ($2\text{--}3 \mu\text{W/m}^3$) are typical of the Proterozoic terranes of the Baltic Shield and the North American craton, and of the Archean-Proterozoic terranes of West Africa, Central Sahara and the southern Africa. Very high values of heat production ($> 5 \mu\text{W/m}^3$) are characteristic of granitic rocks in central Europe, northern Africa (the Syrt Basin) and along the Tasman line in central Australia.

Importantly, granites in many crustal terranes show strong short-wavelength heterogeneity in heat production, such as in the cratons of Australia, India, Tibet, south-eastern China, and southern Baltic shield. We note that strong variations in heat production (by an order of magnitude or more) within rocks of the same lithology have been reported earlier for the Baltic shield (Kukkonen and Lahtinen, 2001).

Radioactive decay leads to a secular decrease in radiogenic heat production in the Earth (Tables 2, 3, Fig. 3), and one would expect that it should also lead to a secular decrease in concentration of radiogenic elements in the continental crust and in the granitic rocks, with the lowest concentration in the older rocks (Fig. 2). In particular, an average post-Archean continental crust should have higher abundances of radiogenic elements than an average Archean continental crust (Table 1), with a 35–40% higher abundances in K, Th, and U.

Our results confirm these earlier findings and indicate that heat production is the lowest in the Archean-Early Proterozoic granitic rocks (Fig. 7). Our database includes data for the granitic rocks of the Early Proterozoic orogens of the Canadian and Baltic Shields, which are characterized by low heat production values (Figs. 5, 8, Table 9).

Importantly, we do not observe a monotonic secular trend (Fig. 7), but instead document a sharp peak of heat production in Middle-Late Proterozoic granites, with a gradual decrease in bulk heat production in granites over the last 2 Gy. We note that a sharp increase in heat production in granitic rocks in the Middle Proterozoic time follows the global-scale collisional events at 2.1–1.8 Ga which were associated with the assembly of the supercontinent Nuna (Columbia) (Zhao et al., 2002). Granites of these ages occur in the Transamazonian and Eburnean Orogenes in South America and West Africa; the Limpopo Belt in southern Africa; the Trans-Hudson, Penokean, Taltson-Thelon, Wopmay, and other Early Proterozoic orogens in North America; the Tasman Fold belt in Australia; the Volyn-Central Russian and Pachelma Orogenes of the East European Craton and the Svecofennian orogen of the Baltic Shield; the Akitkan and Central Aldan Orogenes in Siberia; the Central Indian Tectonic Zone; the Trans-North China Orogen, and the Transantarctic Mountains.

The 2.1–1.8 Ga global-scale collisional event was followed by Middle Proterozoic subduction-related growth along continental margins at 1.8–1.3 Ga (Rogers and Santosh, 2002; Zhao et al., 2004). This resulted in the formation of a great magmatic accretionary belt along the present-day SE margin of North America (the Yavapai-Mazatzal, Labradorian, St. Francois, and Elzevirian Belts), Greenland (the

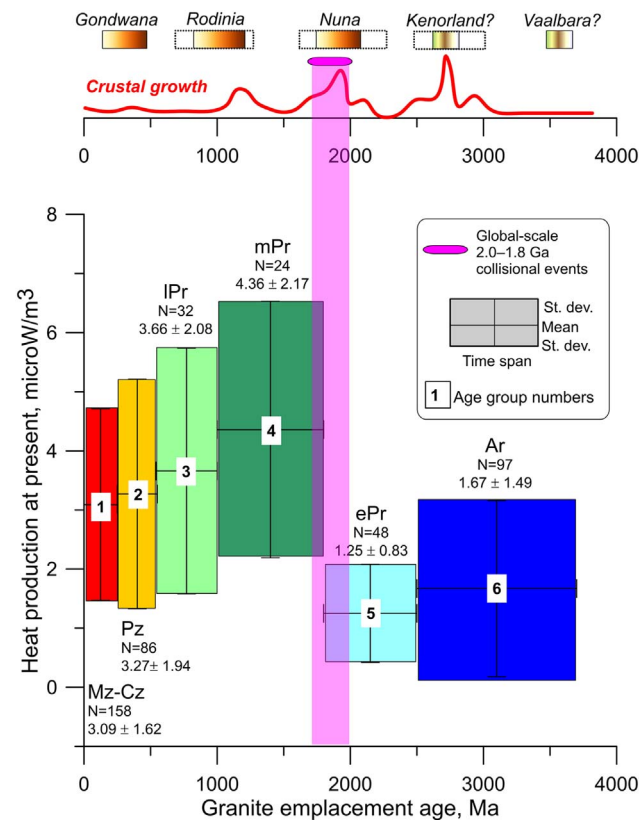


Fig. 7. Present-day heat production in granitic rocks as function of their emplacement age based on the GRANITE2017 database. Horizontal size of colored boxes – time span; vertical size - mean value $\pm 1\sigma$. Red curve on the top – crustal growth (Condé, 1998). A sharp increase in radiogenic heat production in the Middle Proterozoic time may be caused by a global-scale collisional event, possibly related to the supercontinent cycle when changes in the granite forming processes may be expected.

Ketilidian Belt), the Baltic shield (the Transscandinavian Igneous Belt, the Kongsbergian-Gothian, and the SW Sweden Granitoid Belts), the western margin of the Amazonia Craton in South America (the Rio Negro, Juruena, and Rondonian Belts), the SE margins of the North Australia Craton (the Arunta, Mount Isa, and the Georgetown Belts) and the eastern margin of the Gawler Craton (the Broken Hill Belt) in Australia, and the accretionary magmatic belt along the southern margin of the North China Craton (Fig. 5).

Our database has a small number of data for the granitic rocks of the Middle Proterozoic magmatic belts, which are represented by data from the Baltic Shield, the Yavapai-Mazatzal province, the eastern margin of the Gawler Craton, Central India, and the northern margin of the East Saharan craton (Fig. S2). These granitic rocks show a very large range of heat production values with overall very high average values. Many of them have a high concentration of radiogenic elements and therefore high heat production (Fig. 8, Table 9). We next discuss the reasons for the observed global patterns in secular variations in heat production in the granitic rocks, which we link to the Wilson cycle and the tectonic origin of granites.

5.2. Statistical analysis of data

Normal distribution is typical for random variables and we assume that K, U, Th and heat production should follow such distribution, such that 68% of the area lies within 1σ (standard deviation) and 95% lies within 2σ . The outliers usually represent different processes, which in case of heat producing elements may be related to different geodynamic conditions for generation of the granitic magmas or to their later chemical alteration, e.g. by metamorphism, metasomatism, weathering.

Our first-order observation is that bulk heat production in granitic

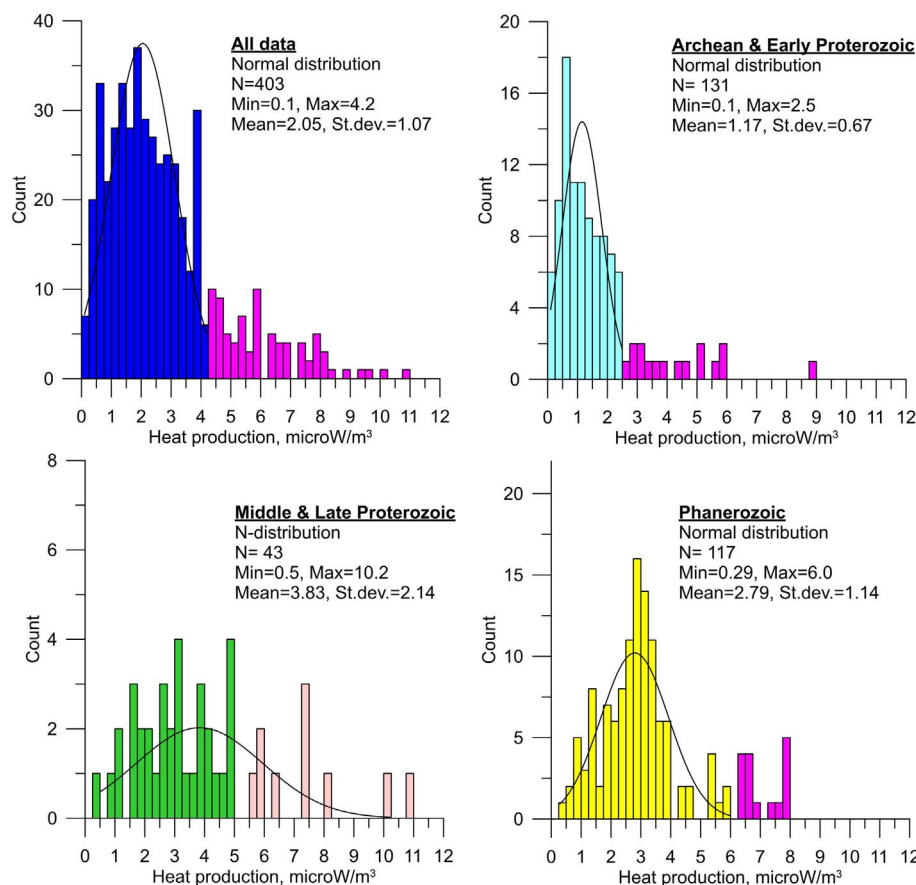


Fig. 8. Statistics for present-day heat production in granitic rocks of different emplacement ages (see Table 6 for details). Age groups for granites are specified in Table 6. Magenta colors show “the tail” beyond ca. 1 σ of the normal distribution, which we attribute to a different mechanism of granitic magmas generation than the normal distribution. Such anomalous tail is typical of Archean-Early Proterozoic granites. It is unclear if Middle-Late Proterozoic granites with $A > 5 \mu\text{W/m}^3$ should be considered as “the tail”. In our analysis we interpret that all granitic rocks of this age belong to the normal distribution.

rocks indeed follows a bell-shaped nearly symmetrical normal distribution when data for all ages are considered (Fig. 8). We have chosen not to fix the value of 1 or 2 standard deviation of the mean to separate variations in heat production related to the dominant and other processes related to the formation and chemical alteration of the granitic rocks (Fig. 8, Fig. S2). Instead, we separated the dominating “normal process” from “the tail” by the A-value where heat production values start forming “the tail”. Such a choice appears to be more justified from geodynamics point of view, given that the various processes responsible for generation of granitic magmas are not fully independent. The cut-off values chosen this way are close to 1 σ and they are essentially

controlled by limitations in the geographical coverage of the database. For example, for granitic rocks of all ages in the database, the mean A value is $2.05 \pm 1.07 \mu\text{W/m}^3$ ($N = 403$) when the outliers with $A > 4.20 \mu\text{W/m}^3$ are excluded (manual choice of the threshold A-value, Fig. 8) and $A = 2.15 \pm 1.17 \mu\text{W/m}^3$ ($N = 398$) for the threshold value of $4.57 \mu\text{W/m}^3$ (one standard deviation of the mean, see Table 9).

By analyzing tectonic settings where the values belong either to the normal distribution or to “the tail” (the outliers), we speculate on major processes responsible for granite formation through the Earth's tectonic history. The results of statistical analysis of granitic rocks of different

Table 9
Average heat production in granites of different ages ($\mu\text{W/m}^3$).

Age of granite emplacement	Phanerozoic		Proterozoic			Archean	
	Meso-Cenozoic	Paleozoic	Late Proterozoic	Middle Proterozoic	Early Proterozoic		
Age group ^a	1	2	3	4	5	6	
GRANITE2017, all data	3.09 ± 1.62 ($N = 158$)	3.27 ± 1.94 ($N = 86$)	4.15 ± 2.26 ($N = 38$)	5.08 ± 2.68 ($N = 14$)	1.45 ± 1.95 ($N = 31$)	1.82 ± 1.57 ($N = 80$)	
GRANITE2017, all data	3.16 ± 1.74 ($N = 244$)		4.40 ± 2.39 ($N = 52$)		1.71 ± 1.68 ($N = 111$)		
GRANITE2017, all data	3.16 ± 1.74 ($N = 244$)		3.30 ± 2.65 ($N = 83$)			1.82 ± 1.57 ($N = 80$)	
Condie, 1993	2.85		2.7			2.3	
Gao et al., 1998	//		2.5			2.3	
GRANITE2017, all data	2.70 ± 1.87 ($N = 456$)						
Vila et al., 2010 (granite)	2.83 ± 2.18 ($N = 309$)						
Vila et al., 2010 (granitoid)	2.52 ± 2.16 ($N = 583$)						

^a Note: the age is here the age of the granite emplacement, not the age of the crustal province. The mean value and standard deviation are based on all data for each age group, in contrast to the values shown in Fig. 8, which refer only to the normal part of the distribution (without the tail).

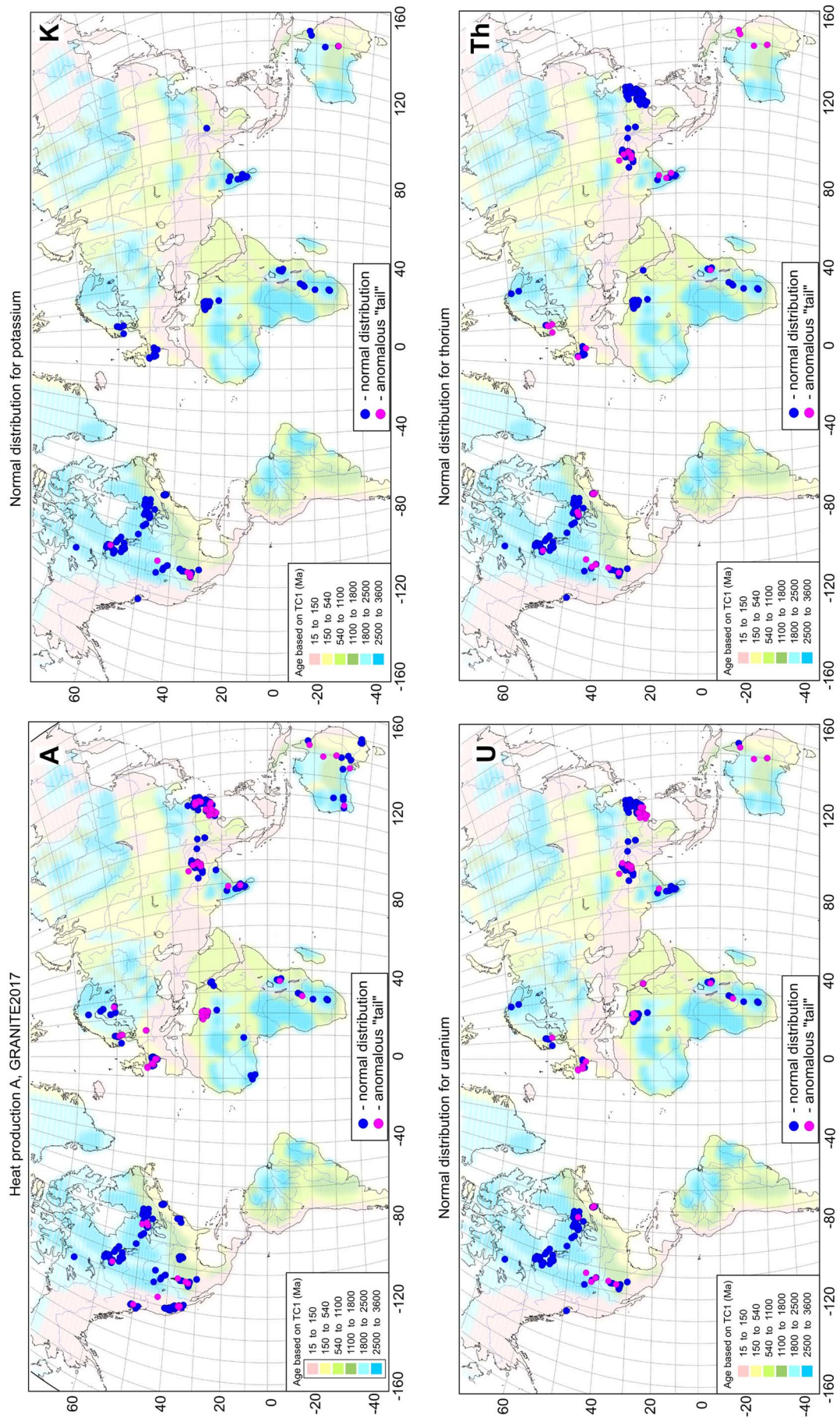


Fig. 9. Map showing location of granitic rocks which follow normal distributions of A, K, Th, and U, and "the tail" which is possibly related to different processes of granite formation. For details see Fig. 8.

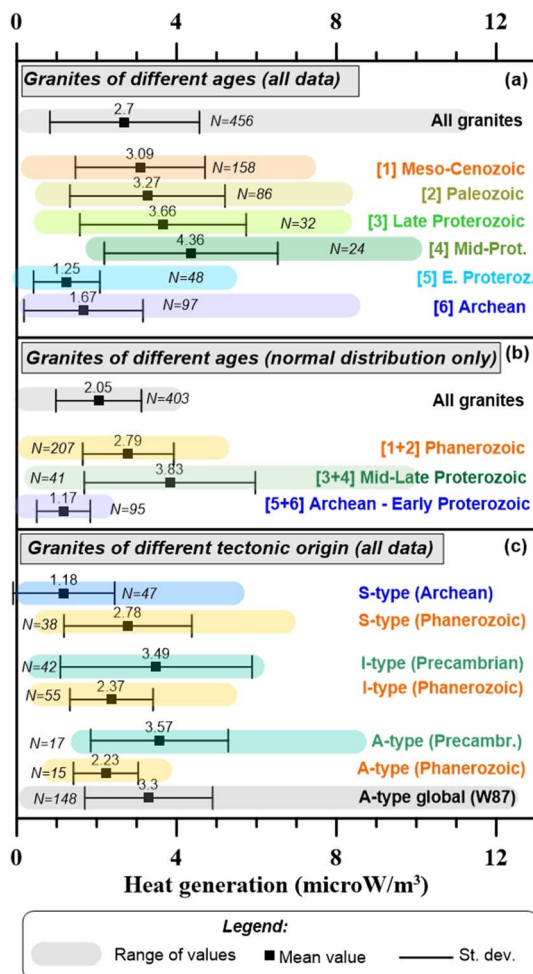


Fig. 10. Summary of heat production in granitic rocks of different emplacement ages and of different tectonic origin. (a) All data versus the emplacement ages; (b) The same as (a) but only for granites that fall within the normal distribution of radiogenic values (Fig. 8); (c) All data versus tectonic origin of granites.

ages are summarized in Table 9 and Figs. 7–10 and they refer to the age of granite emplacement. Note that the statistical values in Table 9 and Figs. 7, 10 are based on all data for each age group, in contrast to the values shown in Fig. 8, which refer only to the normal part of the distribution (without the tail).

The Archean-Early Proterozoic granites have a narrow normal distribution for heat production which is asymmetric towards the values smaller than the mean $A = 1.17 \mu\text{W}/\text{m}^3$ for the normal distribution, with a significant number of values in the range $0.5\text{--}0.8 \mu\text{W}/\text{m}^3$ (Fig. 8). It is possible that two different processes are responsible for the formation of the Archean-Early Proterozoic granites: one produced low-radiogenic granites similar to ocean arc granites (Fig. 1), and the other produced more radiogenic granites. Alternatively, these differences in heat production reflect the degree of later chemical alteration of the Archean-Early Proterozoic granites. In case all data for this age group are included into the statistics, the mean value is $A = 1.76 \pm 1.57 \mu\text{W}/\text{m}^3$ ($N = 160$) when the age corresponds to the granite emplacement age and $A = 2.04 \pm 1.62 \mu\text{W}/\text{m}^3$ ($N = 232$) when the age corresponds to the crustal age.

We speculate that processes of granitic magma generation were more uniform on the early Earth than at later times (Fig. 8), and this is related to both initial magma composition and geodynamic settings for magmatic differentiation processes. Granites of the global 2.1–1.8 Ga collisional event all fall into the normal distribution ($1.45 \pm 1.95 \mu\text{W}/\text{m}^3$, Table 9). The outliers with $A > 2.5 \mu\text{W}/\text{m}^3$ (the tail of the normal distribution for the Archean-Early Proterozoic granites) are rare

(Figs. 8, 9). The anomalously high values are typical of the Archean granites of the southern Superior province, the central Indian shield, the Yilgarn craton, and some parts of Africa where they seem to be related to the East African rift and therefore their age may be significantly younger than assigned based on the crustal age (because no information on the emplacement age is available, Fig. 5).

The Middle-Late Proterozoic granites have a very broad distribution of heat production values, and it is unclear if it may be considered as a normal distribution at all, also considering the relatively low number of entries (58) for this age group (Table 6, Fig. 8). We note that, following the formation of the Nuna supercontinent, many Middle Proterozoic granites have been formed in subduction zones along continental margins such as within the SW Sweden Granitoid Belt and at the SE margins of the North Australia Craton (Fig. S2), while the emplacement of the rapakivi-type granites of southern Baltica may have been caused by mantle upwelling. Therefore, the broad distribution of heat production values reflects the diversity of the tectonic settings where the Middle-Late Proterozoic granites were formed. Importantly, there is a significant difference in heat production between granites formed in the Middle and Late Proterozoic time: Middle Proterozoic granites are unique with an extremely high enrichment in heat producing elements (Fig. 7).

Phanerozoic granites are characterized by a clear normal distribution of heat production values with a more than double mean value ($A = 2.79 \pm 1.14 \mu\text{W}/\text{m}^3$) and a much broader distribution than for the Archean-Early Proterozoic granites (Fig. 8). The large variability of heat production in the Phanerozoic granites reflects compositional variations in magma sources, both in the continental crust and in the mantle, and the diversity of tectonic environments. We do not find any statistically significant difference in heat production between granites formed in the Paleozoic and in the Meso-Cenozoic time (Fig. 7).

6. Heat production in granites and the Wilson cycle

Formation of granites of different types is closely linked to the Wilson cycle (except for some A-type granites at hot-spots, such as e.g. Yellowstone). Importantly, most granitic rocks are formed by melting of several sources (mantle and the crust), which leads to a strong compositional heterogeneity of the granites and a strong variability in concentrations of heat producing elements and bulk rock heat production.

Our original ambition was to examine how the tectonic type (I-type, S-type, and A-type) of granites correlates with concentrations of U, Th and K. Unfortunately, the geochemical information is limited to a general rock type in most publications, making such analysis on a global scale hardly possible. We, nonetheless, assigned the tectonic types to ca. 50% of data, based on the information on a typical type of granites in different tectonic provinces.

The analysis of the relationship between heat production in the granitic rocks and the tectonic environment where the granitic rocks were formed shows that the age of granites is more important than the granite-type in controlling bulk rock heat production (Table 10, Fig. 10). For Phanerozoic granites, we do not find any correlation between the granite type and the A-value. Similarly, the Precambrian I-type and A-type granites have similar values of heat production, which probably can be explained by the differences in how these two types of granites are defined, because technically many A-type granites are I-type. We find, however, that the Precambrian S-type granites are very different from other types and are depleted in heat producing elements. The difference seems to be related to different ages of the Precambrian granites because the S-type granites which we analyzed are Archean, while the Precambrian A- and I-type granites are post-Archean. These Precambrian A- and I-type granites are also the most radiogenic (Fig. 10).

We also examined the correlation between surface heat flow and heat production in granites. Certainly, granitic rocks form only a small

Table 10
Average heat production in different types of granites ($\mu\text{W}/\text{m}^3$).

S-type	I-type	A-type	Location	Ref
1.18 ± 1.27 (N = 47, from 0.1 to 6.0)			Canadian shield (W. Superior)	Present study (Precambrian)
2.78 ± 1.60 (N = 38, from 0.46 to 6.96)			Himalayas	Present study (Phanerozoic)
	3.49 ± 2.40 (N = 42, from 0.40 to 6.0)		Trans-Igneous belt (Baltic Shield), TTG from Indian Shield	Present study (Precambrian)
	2.37 ± 1.04 (N = 55, from 0.29 to 5.45)		Cordillera (W Canada, W USA, NW Mexico)	Present study (Phanerozoic)
		3.57 ± 1.72 (N = 17, from 1.28 to 8.9)	Baltic Shield, Yilgarn	Present study (Precambrian)
		2.23 ± 0.81 (N = 15, from 0.96 to 3.7)	Appalachians	Present study (Phanerozoic)
		3.3 ± 1.6 (N = 148, from 0.52 to 12.7)	Global (?)	Whalen, 1985

portion of the continental crust and other rocks may have a significant contribution to local variations in heat production and heat flow. Furthermore, mantle contribution to surface heat flow (“reduced heat flow” in the concept of “heat flow provinces”) may also be significantly different in different regions. Our analysis does not show any correlation between heat flow and heat production neither for different ages, nor for different types of granites (Fig. 11). There is also no correlation between surface heat flow and concentrations of K, Th, and U in granites, except for a weak correlation between heat flow and K (Fig. S3). Such trend should be expected since potassium is as an essential element of rock-forming minerals (phlogopite, muscovite and biotite) widely present in the granitic rocks, and its contribution to heat production is expected to cause a heat flow increase with an increase of K concentrations. What is more surprising is that the trend is very weak with the strong scatter of data which apparently reflects significant variations in lithology of granitic rocks.

7. Global patterns and secular trends for U, Th, K and their ratios

7.1. Statistical analysis for U, Th, K

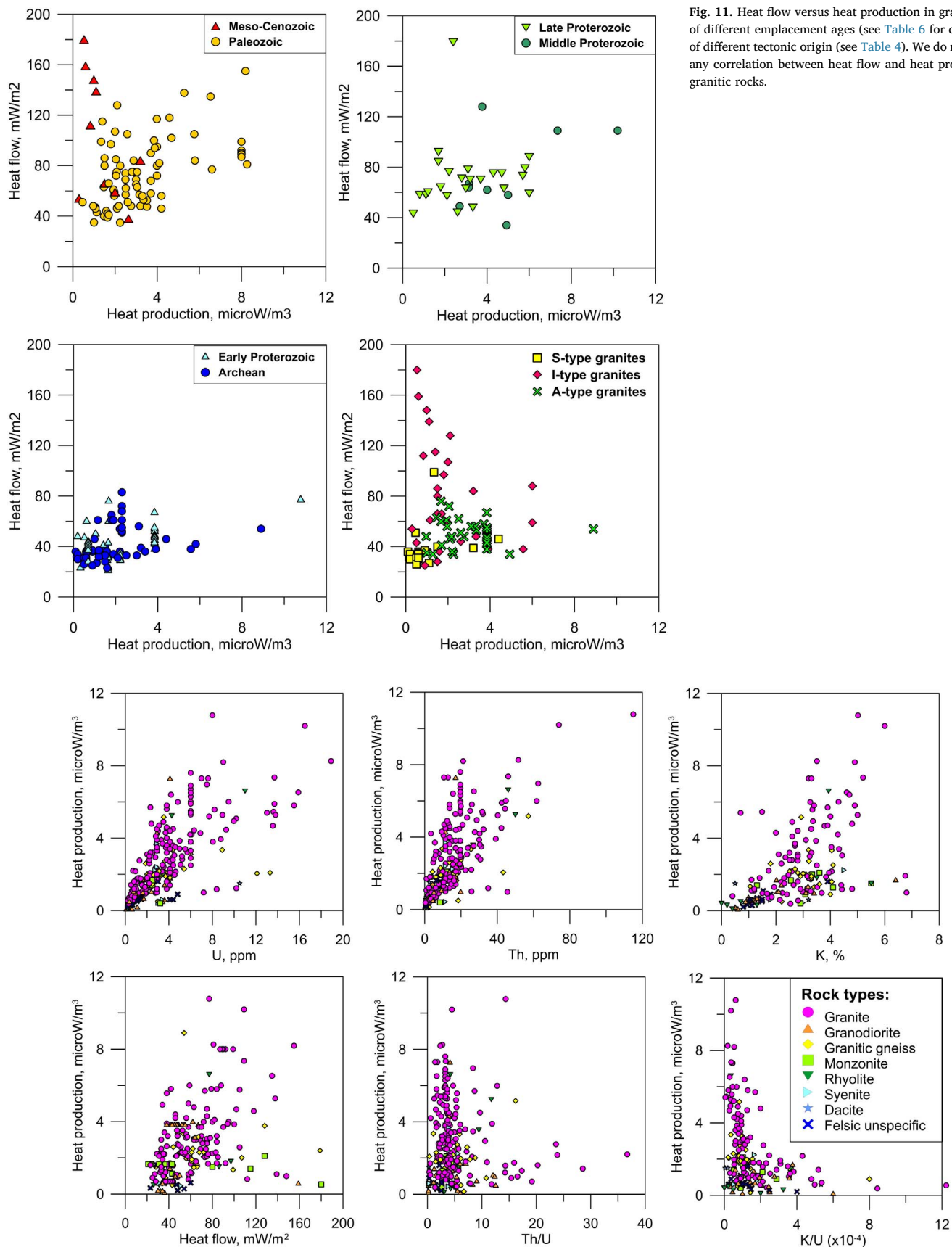
The amount of data on heat producing elements is significantly smaller than for whole rock heat production, in particular for potassium (Table 5). We find that, as expected, an increase in the U and Th concentration in granitic rocks leads, in general, to an increase in heat production (Fig. 12). A similar trend exists for K as well, but the data show a significant scatter. There is no clear correlation between the lithology and heat production in the granitic rocks, although our database is dominated by granites in *sensu stricto*.

We analyze secular variations in heat producing elements in granitic rocks (Figs. 13–16), similar to our analysis of heat production (Fig. 8). The concentration of Th in granitic rocks shows normal distribution for all age groups (Fig. 13) but, similar to the heat production statistics, is essentially asymmetric for Archean and Early Proterozoic granitic rocks with a strong shift towards low values. There is a clear trend towards an increase in concentration of thorium in young granitic rocks (Tables 11–12) and in young crust (Tables 13–14). The outliers with high Th-concentrations all seem to be associated with large-scale collisional events of different ages (Fig. 9) and are typical of the granitic rocks of the Wyoming craton, the Sveconorwegian province of the southern Baltica, the Himalayas, central Australia along the Tasman line, and the Dharwar craton in India.

The uranium concentration shows a pattern similar to Th (Fig. 14) except that, apparently, two different normal distributions may be recognized for Middle-Late Proterozoic granitic rocks, and a similar pattern is observed for potassium (Fig. 15). Granitic rocks with an anomalously high U are in most cases the same as those with an anomalously high Th and, as a result, with a high bulk rock heat production (Fig. 9). Note that the amount of data for potassium in GRANITE2017 is significantly smaller than for U and Th (204 and 307 data entries, respectively; Table 5), and all granitic rocks with an anomalously high potassium seem to be younger than 1.8 Ga (Fig. 15).

As a general trend, concentrations of Th, U and K typically are low in the Archean-Early Proterozoic granitic rocks (Fig. 16). Low heat production in the old continental blocks may, among other things, be important for their preservation in the geological record.

There is a marked increase in concentration of all three radiogenic elements from Archean-Early Proterozoic to Middle Proterozoic age, although the GRANITE2017 database includes relatively few data for this age and the peak associated with Middle Proterozoic granites may be an artifact caused by possible non-representativeness of the data. However, we consider a significant difference between Archean-Early Proterozoic granitic rocks and younger rocks as a robust result which reflects global patterns. We speculate that the assemblage of the Early Proterozoic supercontinent changed globally the geodynamic environment for the generation of granitic rocks. The Early Proterozoic granites



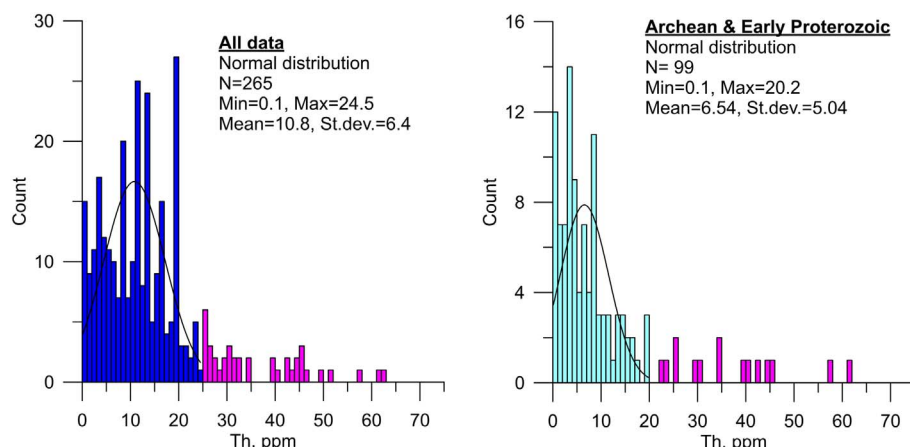


Fig. 13. Statistics for present-day Th concentration in granitic rocks of different emplacement ages (see Table 6 for details). Magenta shows “the tail” beyond ca. 1σ of the normal distribution, which we attribute to mechanisms of granitic magmas generation other than the one responsible for the normal distribution. Such anomalous tail is observed for granitic rocks of all ages. For Archean-early Proterozoic granites, a significant number of samples has a very low concentration of Th, suggesting that they may have also been formed under different conditions.

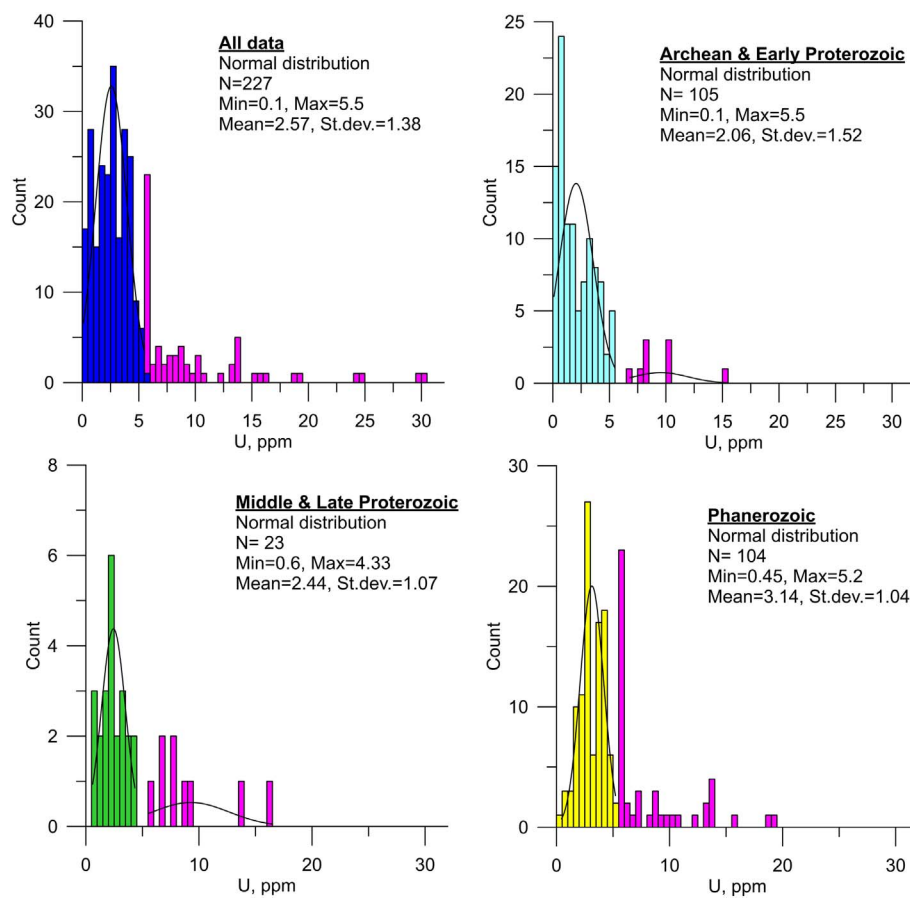
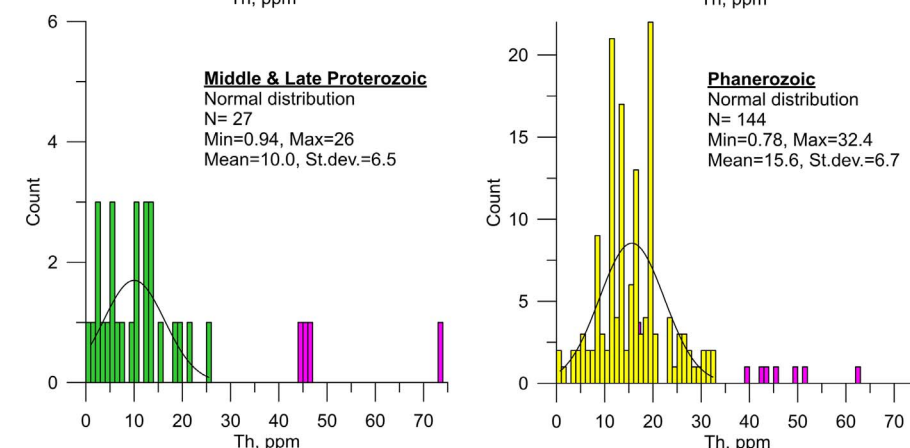


Fig. 14. Statistics for present-day U concentration in granitic rocks of different emplacement ages. Magenta shows “the tail” which we attribute to a different mechanism of granitic magmas generation than the normal distribution. Such anomalous tail is observed for granitic rocks of all ages. For Archean-early Proterozoic granites, a significant number of samples has a very low concentration of U, suggesting that they may have also been formed under different conditions.

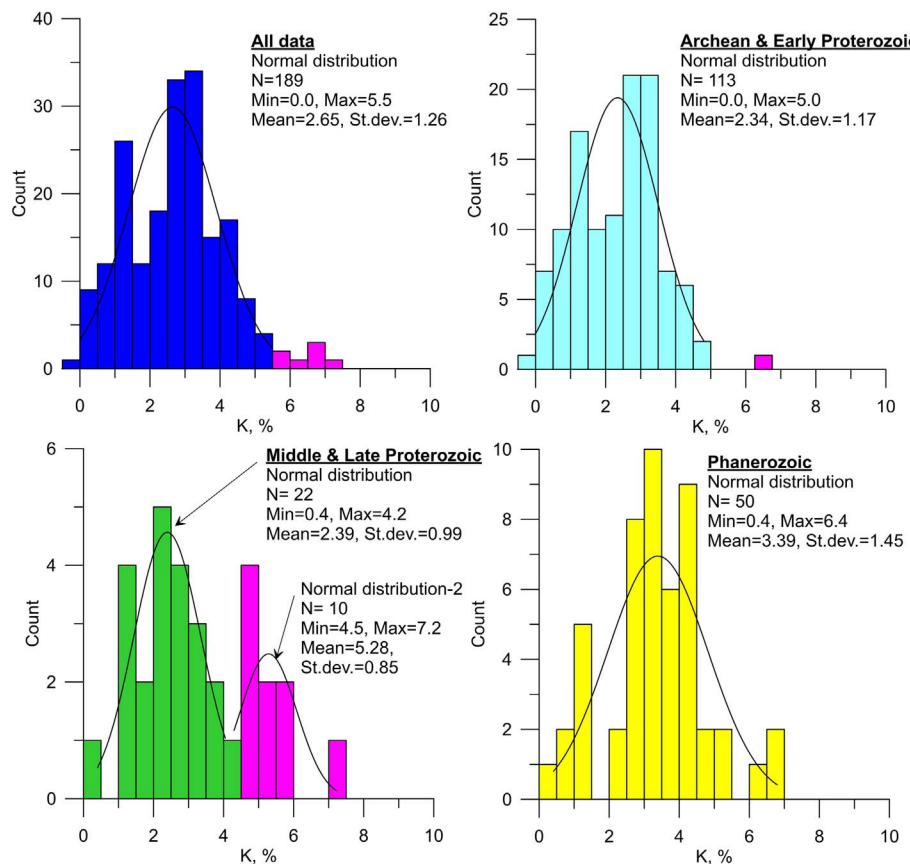


Fig. 15. Statistics for present-day K concentration in granitic rocks of different emplacement ages. Magenta shows “the tail” which we attribute to a different mechanism of granitic magmas generation than the normal distribution. Such anomalous tail is typical mostly of the Middle and Late Proterozoic granitic rocks. The amount of data for K concentrations in granites is smaller than for Th and U (Table 5).

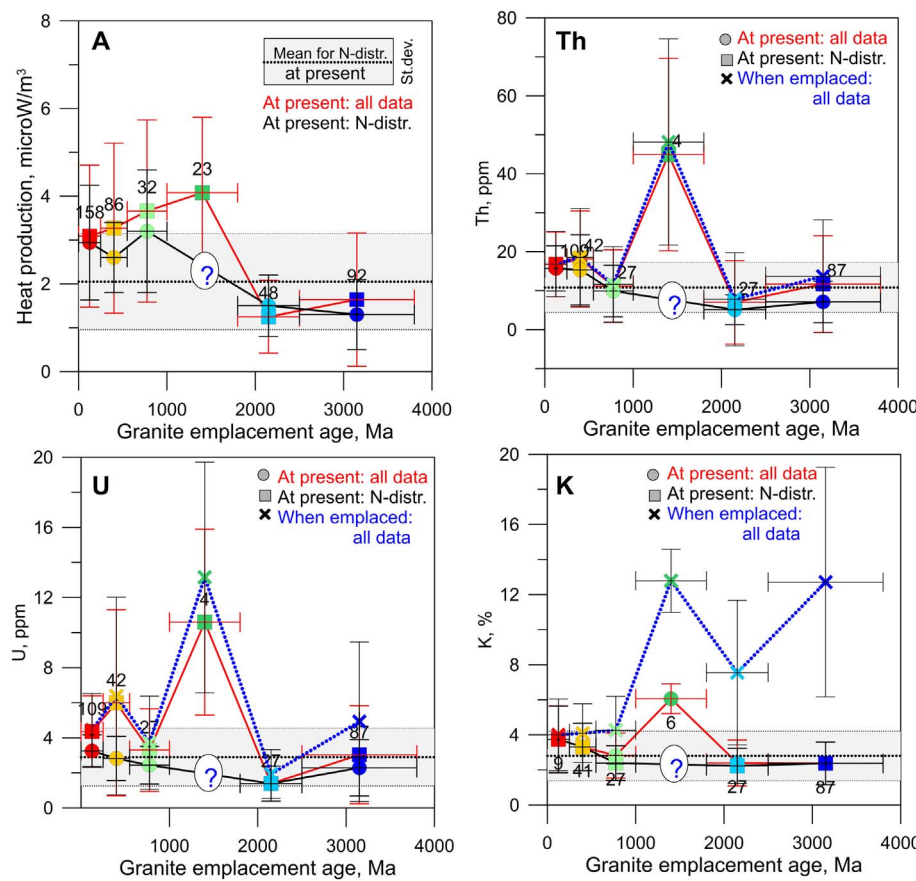


Fig. 16. Average values of present-day heat production A and concentrations of U, Th, K for granitic rocks of different emplacement ages (see Tables 11–12 for details and Table 6 for age group definition). Red lines – based on all data in the GRANITE2017 database; black lines – only for the present-day values that follow normal distributions (for details see Figs. 8, 13–15); blue lines – for all data in the database recalculated to the time of the granite emplacement (age taken as the mid-age for each geological epoch). Vertical lines – standard deviation. Gray boxes - the mean values for normal distribution (shown by dotted lines) $\pm 1\sigma$.

Table 11

Present-day variations in heat producing elements (normal distribution only) for granites of different emplacement ages.

Age of granite	A total ^a , $\mu\text{W}/\text{m}^3$	Th, ppm	U, ppm	K, %	Th/U	$\text{K}/\text{U} \times 10^4$
Phanerozoic (groups 1 + 2)	2.79 ± 1.14	15.6 ± 6.7	3.13 ± 1.04	3.39 ± 1.45	3.89 ± 1.55	0.88 ± 0.60
Middle and Late Proterozoic (groups 3 + 4)	3.83 ± 2.14	10.0 ± 6.5	2.44 ± 1.07	2.39 ± 0.99	3.63 ± 1.95	0.98 ± 0.44
Archean and Early Proterozoic (groups 5 + 6)	1.17 ± 0.67	6.5 ± 5.0	2.06 ± 1.52	2.34 ± 1.17	3.50 ± 2.18	1.16 ± 0.71
All ages	2.05 ± 1.07	10.8 ± 6.4	2.57 ± 1.38	2.65 ± 1.26	3.68 ± 1.84	0.93 ± 0.53

^a Based on the average for the complied published data. In case Th, U, and K data from the Table are used, Eq. (1) yields 1.66 $\mu\text{W}/\text{m}^3$. The difference is due to the fact that GRANITE2017 database has incomplete information for K (Table 5).

are characterized by narrow normal distributions of the concentrations of radiogenic elements (and bulk rock heat production) suggesting a similar geodynamic origin of granitic magmas. In contrast, Middle Proterozoic granites were produced in accretional magmatic belts and subduction zones at the margins of the supercontinent as well as, possibly, in intracratonic settings by mantle plumes. As a result, they show an extreme diversity of concentrations of radiogenic elements and a marked increase in their concentrations which suggests that a significant part of Middle Proterozoic granites was formed with involvement of large volumes of mantle material.

Surprisingly, the mean values for the normal distributions of Th, U, and K are extremely close to the abundances of these radioactive elements in the average upper continental crust as reported by van Schmus (1995) (compare Table 1 and Figs. 13–15). In contrast, USGS granite (Table 1) is much more radiogenic than the average for our data compilation, and rather corresponds to the highly radiogenic “tail” in data than to “normal” granite.

7.2. Implications for Precambrian thermal evolution and plate motions

We calculate concentrations of U, Th, and K at different geological times in the past (at the time of granite emplacement) (Figs. 16–17), using data on the present day concentrations of heat producing elements in granites of different emplacement ages (Table 14 and Fig. 16) and data on the half-life of heat producing isotopes (Table 2). As expected, their concentrations increase with age (Fig. 17). We use these data to calculate secular variations in average heat production in granitic rocks (see Section 3.2) (Fig. 18). Importantly, we do not observe a monotonous general decrease in heat production in granitic rocks since the Archean, as it has been reported for the bulk Earth based on geochemical models of the Earth's composition (Fig. 3). Note that our results apply only to the granitic crust which makes < 0.2% of the bulk silicate Earth (BSE) mass and < 0.1% of the whole Earth's mass.

The results (Fig. 18) confirm our earlier conclusion (Fig. 7) which shows the present-day heat production in granitic rocks emplaced at different ages) that the Middle Proterozoic granitic rocks had an extremely high concentration of U, Th, and K, and they probably were produced under significantly different conditions than older and younger granitic rocks. Note that in contrast to Fig. 18, the present-day heat production in Fig. 7 was not calculated from concentrations of U, Th, and K in the database, but instead we used heat production values reported in literature because of their larger number.

A sharp increase in the partitioning of heat producing elements into

the Middle Proterozoic granites may have led to a change in the Urey ratio (the ratio of total heat production to the total surface heat flow), which is strongly dependent on the internal heating rate in the mantle caused by heat production and partitioning of heat-producing elements from the mantle into the crust through mantle melting and magmatism (Nakagawa and Tackley, 2012). The Urey ratio controls the thermochemical evolution of the mantle and the vigor of mantle convection. However, until present it is poorly constrained, and geochemical and mantle convection models place significantly different bounds on its value, from 0.08 to 0.49 and > 0.5, respectively (Jaupart et al., 2007; Korenaga, 2008; Deschamps et al., 2010; Nakagawa and Tackley, 2012). Although our results do not directly constrain the Urey ratio, they provide strong evidence that it had a non-monotonic secular change.

There is an intriguing agreement between our model for the average heat production in the past (Fig. 18) and the global average plate velocity model (Korenaga, 2006): fast plate velocities correlate with high heat production in granites. We speculate that fast moving plates promote a higher intensity of collisional tectonics which, in turn, provide favorable conditions for the generation of granitic rocks. The Middle Proterozoic maximum in plate velocities and heat production also corresponds to the minimum predicted lithosphere plate thickness (Korenaga, 2006), therefore supporting our conclusion on a significant change in the mantle convection style and reorganization of the plate tectonics style in Middle Proterozoic. A change in heat production reflects a change in mantle melting conditions for granite generation. This, in turn, reflects changes in mantle potential temperature and, as a result, changes in the depth of mantle melting, volume and composition of generated magmas, as well as changes in temperature-dependent viscosity which controls the vigor of mantle convection and the velocities of plate motions. High concentration of heat producing elements suggests a broader involvement of deeper mantle reservoirs, which may indicate a significant large-scale reorganization of mantle convection (possibly more rigorous), which in turn may have led to faster plate tectonics.

The positive feedback between secular variation in the average heat production in granitic rocks (Fig. 18) and the globally average plate velocity suggests that scaling of global heat production may be used to make robust predictions for global plate velocities in the past. Our model indicates that heat production in the Archean was twice the Early Proterozoic heat production, and it therefore supports a broadly accepted hypothesis of faster plate tectonics in the Archean (e.g. Abbott et al., 1994). Concurrently with a sharp increase in heat production,

Table 12

Present-day variations in heat producing elements (all data) for modern granites of different emplacement ages.

Age of granite	A total ^a , $\mu\text{W}/\text{m}^3$	Th, ppm	U, ppm	K, %	Th/U	$\text{K}/\text{U} \times 10^4$
Phanerozoic (groups 1 + 2)	3.16 ± 1.74	17.12 ± 9.60	4.81 ± 3.34	3.39 ± 1.45	4.17 ± 2.54	1.11 ± 0.96
Middle and Late Proterozoic (groups 3 + 4)	4.40 ± 2.39	18.8 ± 24.65	4.49 ± 3.81	3.38 ± 1.67	3.78 ± 2.69	0.99 ± 0.45
Archean and Early Proterozoic (groups 5 + 6)	1.71 ± 1.68	10.6 ± 12.1	2.65 ± 2.60	2.38 ± 1.23	5.75 ± 5.96	1.75 ± 1.84
All ages	2.70 ± 1.87	14.8 ± 13.2	3.93 ± 3.27	2.79 ± 1.44	4.75 ± 4.27	1.46 ± 1.53

^a Based on the average for the complied published data. In case Th, U, and K data from the Table are used, Eq. (1) yields 2.30 $\mu\text{W}/\text{m}^3$. The difference is due to the fact that GRANITE2017 database has incomplete information for K (Table 5).

Table 13

Present-day variations in heat producing elements in granites (normal distribution only) for crustal provinces of different ages.

Age of crustal province	Th, ppm	U, ppm	K, %	Th/U	K/U × 10 ⁴
Phanerozoic (groups 1 + 2)	17.3 ± 5.5	5.14 ± 2.80	3.68 ± 1.13	3.82 ± 1.24	0.97 ± 0.61
Middle and Late Proterozoic (groups 3 + 4)	11.8 ± 7.5	2.58 ± 1.10	3.24 ± 1.44	3.26 ± 1.79	0.86 ± 0.54
Archean and Early Proterozoic (groups 5 + 6)	8.50 ± 5.4	2.38 ± 1.45	2.45 ± 1.35	3.79 ± 1.97	1.16 ± 0.79

Table 14

Present-day variations in heat producing elements (all data) in granites for crustal provinces of different ages.

Age of crustal province	Th, ppm	U, ppm	K, %	Th/U	K/U × 10 ⁴
Phanerozoic (groups 1 + 2)	18.1 ± 7.20	5.14 ± 2.8	3.68 ± 1.13	4.12 ± 2.73	1.20 ± 0.97
Middle and Late Proterozoic (groups 3 + 4)	15.9 ± 14.4	6.62 ± 7.35	3.24 ± 1.43	3.33 ± 2.63	0.97 ± 0.76
Archean and Early Proterozoic (groups 5 + 6)	12.9 ± 13.7	3.15 ± 2.62	2.44 ± 1.33	5.23 ± 4.91	1.70 ± 1.80

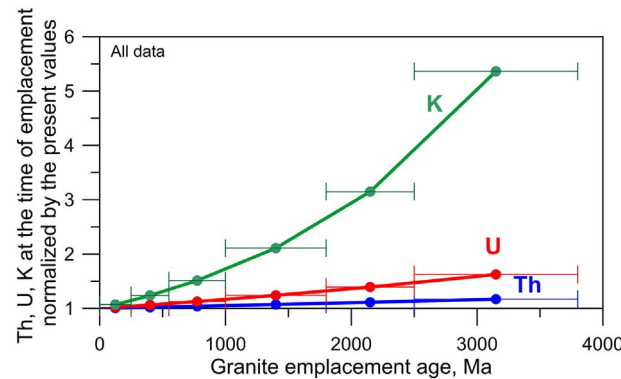


Fig. 17. Secular variations in concentrations of U, Th, K for granitic rocks of different emplacement ages.

past plate motions significantly accelerated in the Middle Proterozoic and then significantly slowed down since the Late Proterozoic.

7.3. Statistical analysis for Th/U and K/U ratios

It has long been proposed that the expected global mean planetary ratios are 3.7–4.0 for Th/U and ca. 10,000 for K/U (Taylor and McLennan, 1985). Later studies reveal a significant variability of the K/U ratio for the bulk Earth, primitive mantle and continental crust, with commonly accepted K/U values for the continental crust of $12,400 \pm 4900$ (Rudnick and Gao, 2003). The highest K/U estimates were reported for the depleted MORB mantle and back-arc basin basalts, $19,000 \pm 2600$ and $21,700 \pm 2000$, respectively (Arevalo et al., 2009). The reported values for the Th/U ratio in the bulk continental crust also has a significant range from 3.8 (McLennan, 2001) to 5.2–5.3 (Wedepohl, 1995; Hacker et al., 2011).

Regional processes may cause selective reduction in concentrations of the heat producing isotopes, in particular uranium. This would result in high values of the Th/U and K/U ratios and one might expect a negative correlation between the isotope ratios and heat production. However, we do not observe this trend in our data (Fig. 12) and therefore conclude that uranium leaching has not substantially affected the granite rocks included into this compilation.

Our analysis indicates that for granitic rocks which follow the normal distribution of heat producing elements and heat production, the ratios Th/U and K/U are close to the proposed global mean ratios (Tables 11, 13). The mean values, however, disregard the highly radioactive “tail” (Figs. 19–20), and when these anomalous data are included into the calculations, the global mean values for granitic rocks are markedly higher (Tables 12, 14), although the sampling is very uneven and not fully global. The geographical distribution of regions with anomalous ratios is different for Th/U and K/U (Fig. 21), and we

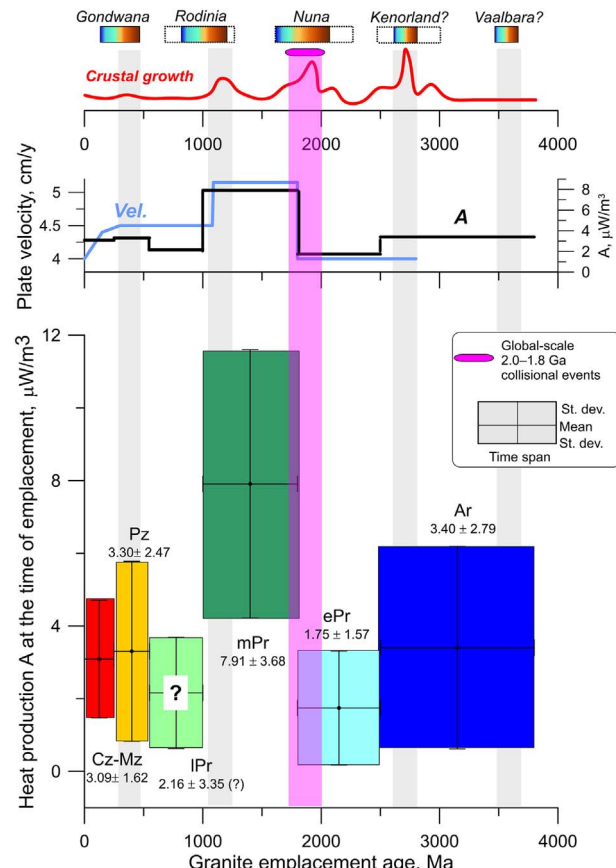


Fig. 18. Heat production in granitic rocks at the time of their emplacement based on the GRANITE2017 database (see Table 15 for details and compare with Fig. 7). Horizontal size of colored boxes – time span; vertical size - mean value $\pm 1\sigma$.

On the top: red curve – crustal growth (Condie, 1998); color boxes – supercontinents. Pink shading corresponds to a global-scale Middle Proterozoic collisional event; gray shadings – collisional events associated with the assemblage stage of other supercontinent. We propose that the Middle Proterozoic peak in heat production in granites may be related to the supercontinent cycle with a change in the granite forming processes.

In the middle: black line – mean values of heat production (shown at the bottom plot); blue line – globally average plate velocity (Korenaga, 2006), assuming the Urey ratio of 0.15–0.30. Plate velocity model is constrained assuming nearly constant intervals of ~800 Myr for the Wilson cycles. Therefore plate velocities prior to a ~2.7 Ga supercontinent are not constrained.

note again that we have a limited amount of data for K abundances in the database.

It is important that anomalously high ratios of Th/U (> 10) and K/U ($> 30,000$) all seem to be restricted to Archean – Early Proterozoic granitic rocks (Figs. 19–21). For “normal” data only, there seem to be a

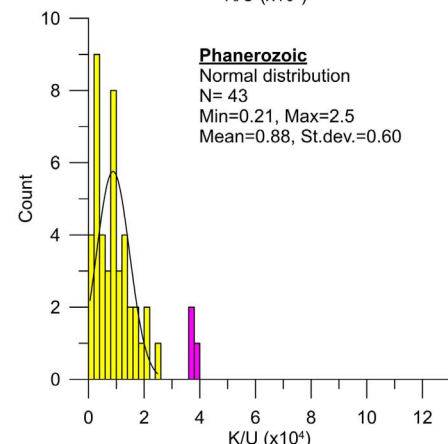
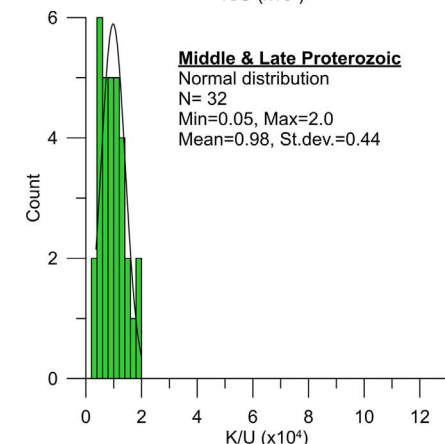
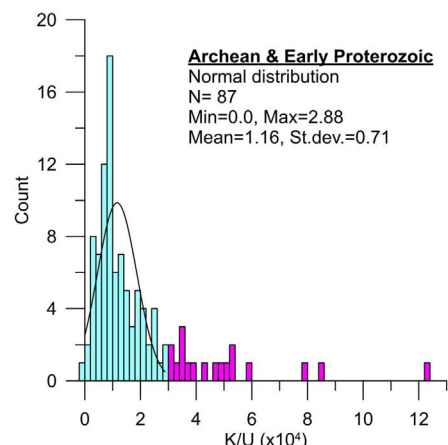
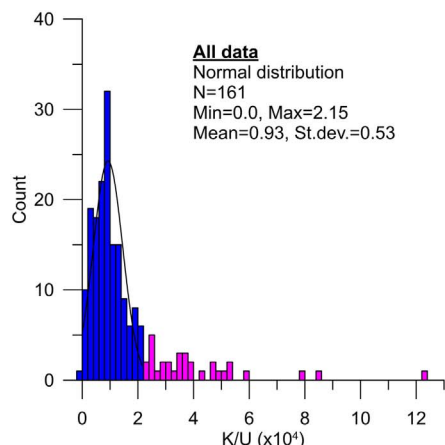
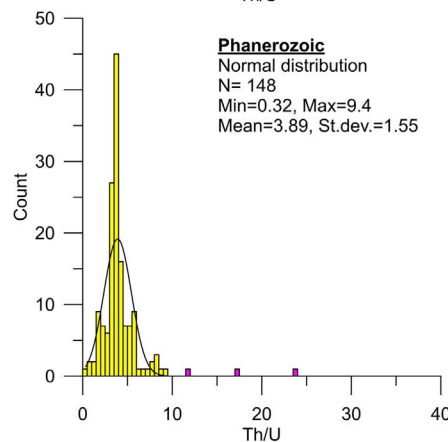
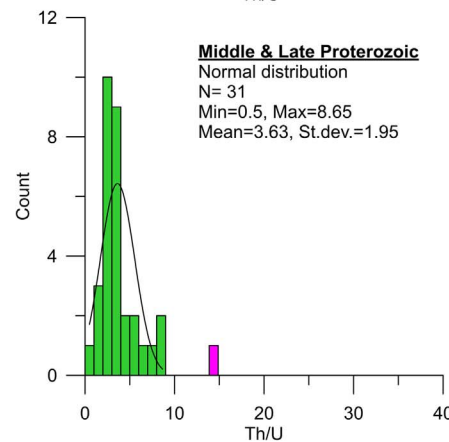
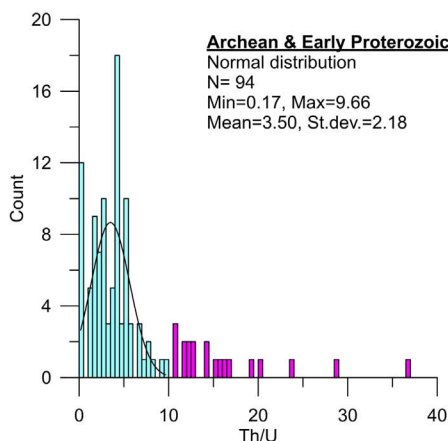
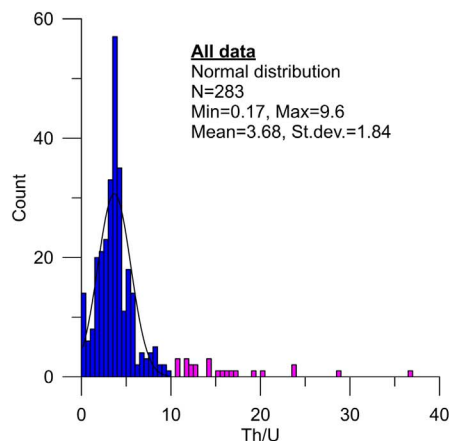


Fig. 19. Statistics for Th/U ratio in granitic rocks of different emplacement ages. Magenta shows “the tail” which we attribute to a different mechanism of granitic magmas generation than the normal distribution. Such anomalous tail is typical mostly of the Archean - Early Proterozoic granites.

Fig. 20. Statistics for K/U ratio in granitic rocks of different emplacement ages. Magenta shows “the tail” which we attribute to a different mechanism of granitic magmas generation than the normal distribution. Such anomalous tail is typical mostly of the Archean-early Proterozoic granites.

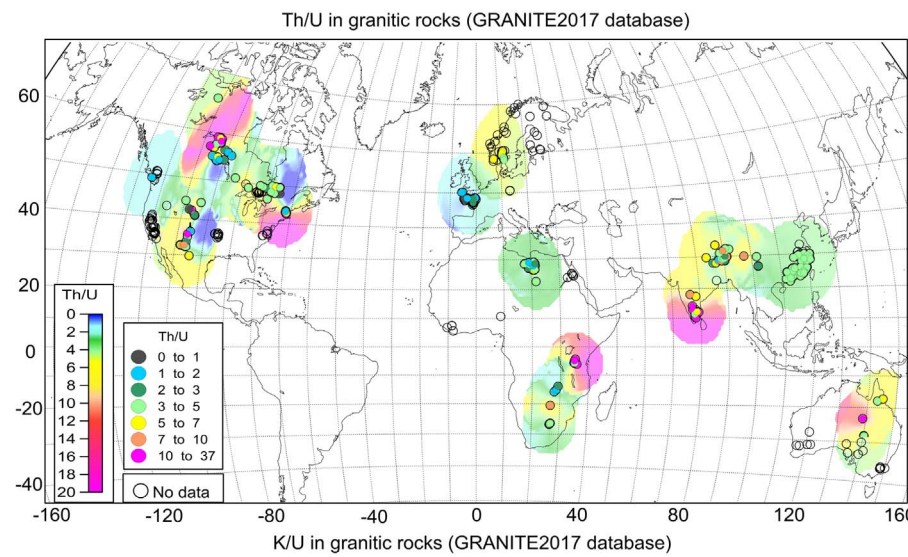


Fig. 21. Distribution of the Th/U and K/U ratios in granitic rocks worldwide.

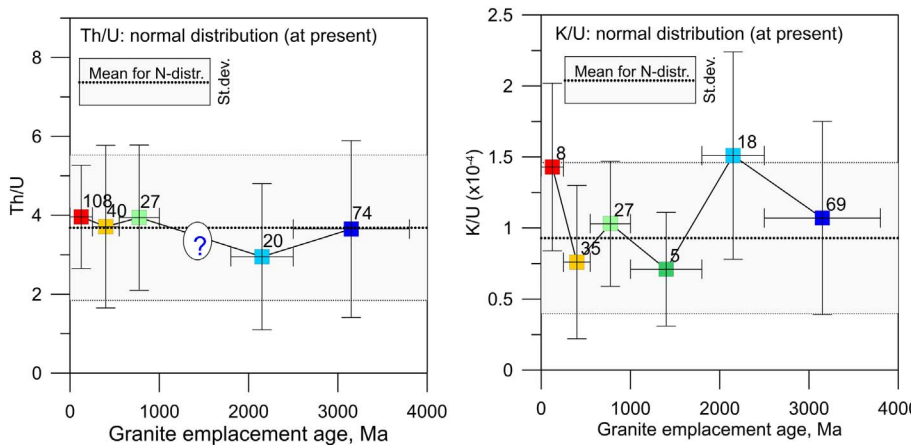
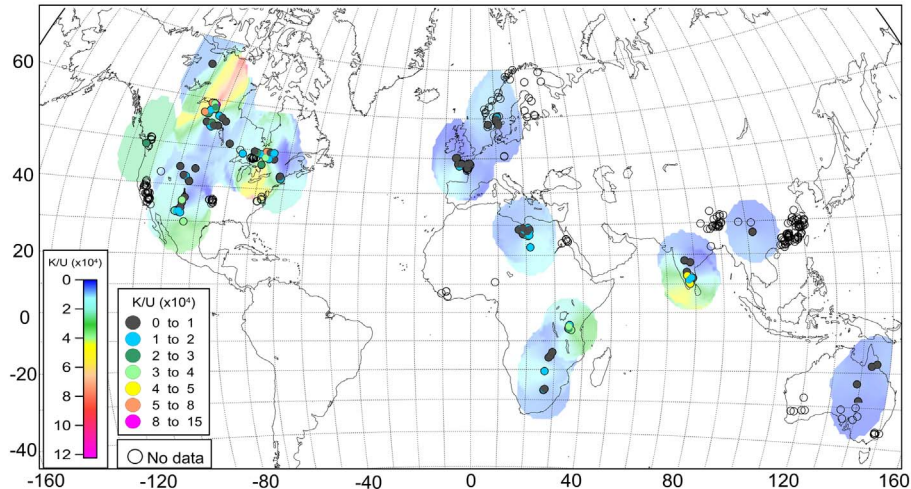


Fig. 22. Present-day Th/U and K/U ratios in granitic rocks versus emplacement ages (see Table 11 for details and Table 6 for age group definition). Symbols (numbers show the number of data points) and black lines – for data that follows normal distributions (for details see Figs. 19–20). Vertical lines – standard deviation. Gray boxes - the mean values for normal distribution (shown by dotted lines) $\pm 1\sigma$.

weak general increase of the Th/U ratio and a decrease of the K/U ratio from older to younger granites (Fig. 22) (except for Meso-Cenozoic granites), in agreement with expectations from secular changes in the abundances of the radiogenic elements (Fig. 3). However, the data show a huge scatter (Fig. 23, Figs. S5, S6).

Based on results presented in Fig. 16, we calculate secular variations in the Th/U and K/U ratios (Fig. 24). We do not observe monotonous trends as predicted for the bulk Earth based on geochemical models of composition (Fig. 3). Our results are in agreement with the global

estimate of ca. 12,400 for the continental crust (Rudnick and Gao, 2003) only for the entire dataset, but in disagreement with the global ratio for each geological time (Table 15). Overall, the K/U ratio is close to 10,000 only for granitic rocks emplaced since ca. 1.8 Ga (Fig. 24), while Archean and, in particular, Early Proterozoic granites have extremely high K/U ratios of ca. 26,000–39,000 due to high concentration of potassium (Fig. 16). The values for the Paleozoic minimum in the K/U ratio (6400) are close to the estimates of a silicate Earth K/U ratio of 7000 to 9000 (Lassiter, 2004) and are consistent with several other

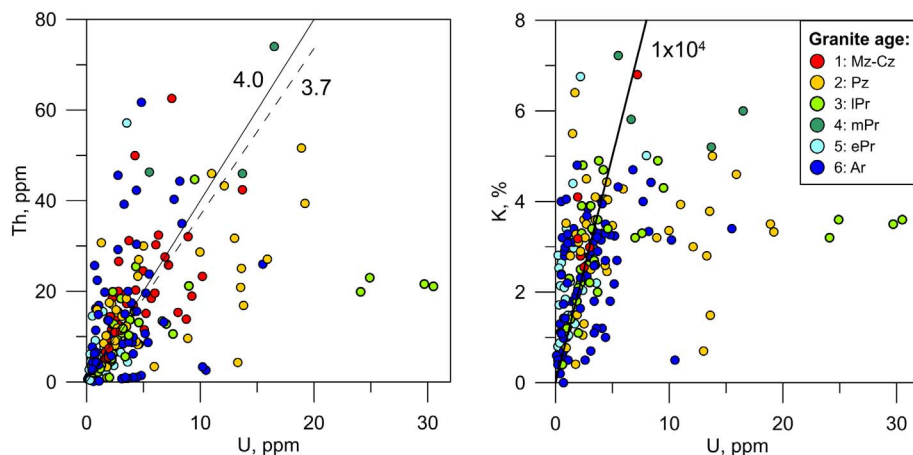


Fig. 23. Correlations between Th, K and U. Colors refer to different granite emplacement ages.

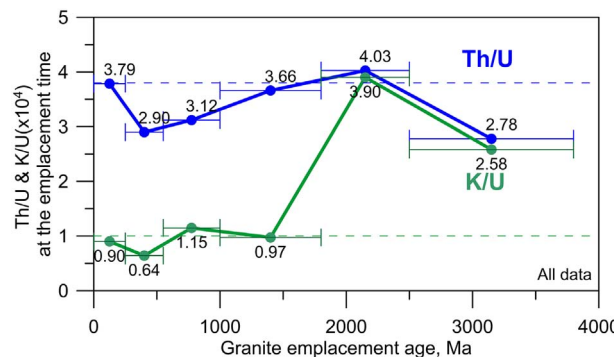


Fig. 24. Th/U and K/U ratios in granitic rocks at the time of emplacement (compare with Fig. 22, for details see Table 15).

models which suggest a K/U ratio in the silicate Earth of ca. 6000–7000 (Albarède, 1998; Davies, 1999).

The Th/U ratio exhibits a subtle decrease from Early Proterozoic to Paleozoic granites (Fig. 24), with the opposite trend of the bulk Earth (Fig. 3). The most prominent feature is a sharp minimum ($\text{Th}/\text{U} \sim 2.78$) in the Archean caused by a high amount of U in granites emplaced at that time. This value is significantly lower than the Th/U ratios reported in literature.

We also examine the variation of the Th/U ratio in granites of different tectonic origin (Fig. 25) and compare them with published data. Our results suggest that the Th/U ratio does not depend on the tectonic type of the granite, whereas granite age seems to be a much stronger controlling factor. However, we note that the I-type Archean granitic rocks seem to have the highest Th/U ratio.

We also analyze the effect of composition of granitic rocks on heat production, concentrations of radiogenic elements, and their ratios (Fig. 26). Based on data in the GRANITE2017 compilation, granites *sensu stricto* have the highest Th and U abundances and highest heat production compared to other felsic rocks. However, our database is dominated by granites and therefore the conclusion may not be robust.

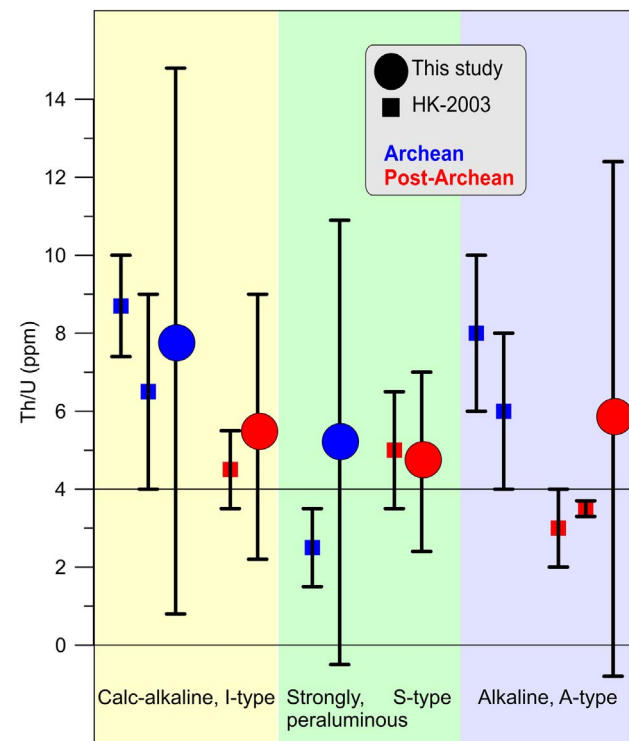


Fig. 25. Th/U ratio for the Archean (blue symbols) and post-Archean (red symbols) granitic rocks of different composition and origin. Circles – based on the GRANITE2017 database; rectangles - based on Kemp and Hawkesworth (2003). Our data does not show any systematic difference between Archean and post-Archean granites. Compare with Fig. 22.

8. Summary and conclusions

Our statistical analysis of a new global database GRANITE2017 on the abundances of heat producing elements (Th, U, K) and heat

Table 15
Secular variations in heat producing elements (all data) at the time of granite emplacement.

Emplacement time ^a	A, $\mu\text{W}/\text{m}^3$	Th, ppm	U, ppm	K, %	Th/U	K/U
Meso-Cenozoic (125 ± 125 Ma)	3.1 ± 1.0	16.8 ± 8.4	4.4 ± 2.1	4.0 ± 2.0	3.78	9000
Paleozoic (400 ± 150 Ma)	3.3 ± 2.5	18.5 ± 12.6	6.4 ± 5.6	4.1 ± 1.7	2.90	6400
Late Proterozoic (775 ± 225 Ma)	2.2 ± 1.5	11.6 ± 9.7	3.7 ± 2.7	4.3 ± 1.9	3.12	11,500
Middle Proterozoic (1400 ± 400 Ma)	7.9 ± 3.7	48.1 ± 26.5	13.2 ± 6.6	12.8 ± 1.8	3.67	9700
Early Proterozoic (2150 ± 350 Ma)	1.7 ± 1.6	7.8 ± 11.9	1.9 ± 1.4	7.6 ± 4.1	4.03	39,000
Archean (3150 ± 650 Ma)	3.4 ± 2.8	13.7 ± 14.5	4.9 ± 4.5	12.7 ± 6.5	2.78	25,800

^a Values used in calculation of Th, U, and K concentrations in the past.

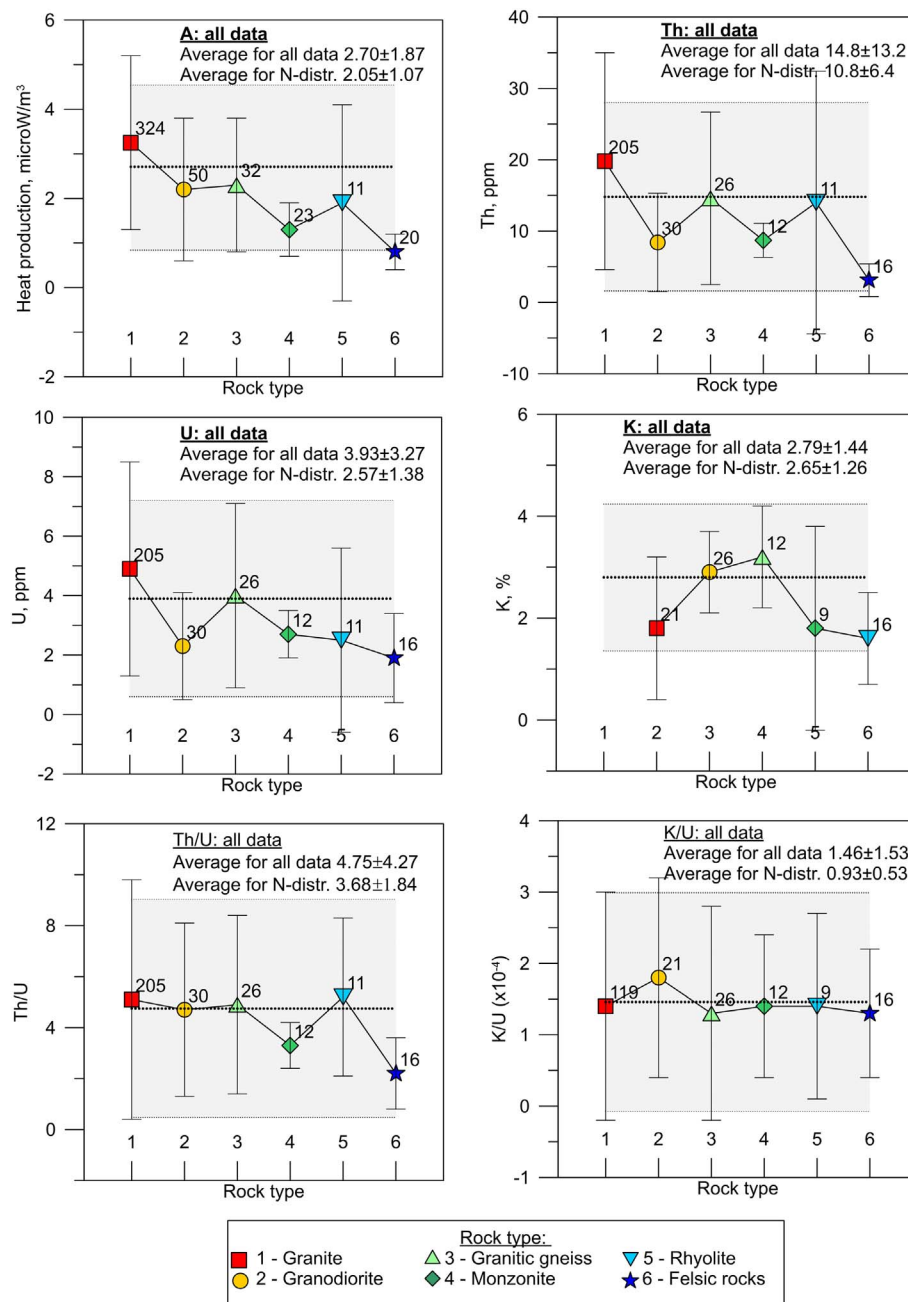


Fig. 26. Heat production A, concentrations of U, Th, K and Th/U and K/U ratios in granitic rocks of different composition (see legend at the bottom for notations). Vertical lines – standard deviation, numbers show the number of data points. Dotted black lines – mean value for all data, gray boxes show the mean $\pm 1\sigma$. See Tables 11–12 for details.

production (A) in granitic rocks has revealed the following major patterns:

1. Granitic rocks show strong short-wavelength heterogeneity of heat production and abundance of heat producing elements with strong variation in the values by an order of magnitude or more. A-type Precambrian granites are the most radioactive, but there is no systematic correlation between the tectonically controlled granite-type (S-, A-, or I-type) and bulk heat production. Instead the age of granites appears more important for heat production.

We do not observe any correlation between heat flow and heat production in granites (Fig. 11). There is also no correlation between surface heat flow and concentrations of K, Th, and U in granites, except for a weak correlation between heat flow and K abundances.

2. Young granitic rocks have the highest heat production and

concentrations of Th, U and K for the normal distribution subset (Fig. 27). For all data there is almost no difference in the concentrations of Th, U and K between Middle-Late Proterozoic and Phanerozoic granites.

All granitic rocks with an anomalously high K-concentration seem to be younger than 1.8 Ga. All granites with high Th-concentrations seem to be associated with large-scale collisional events of different ages. Granitic rocks with an anomalously high Th-concentrations usually also have anomalously high U-concentrations and, as a result, a high bulk rock heat production.

3. Abundances of Th, U, K, values of A, and the ratios Th/U and K/U show bell-shaped normal distributions for the majority of data, but up to 30% of the data form “tails” with significantly higher values (outside 1σ of the mean) (Fig. 27). We interpret these “tails” as reflecting special geodynamic environments for the generation of

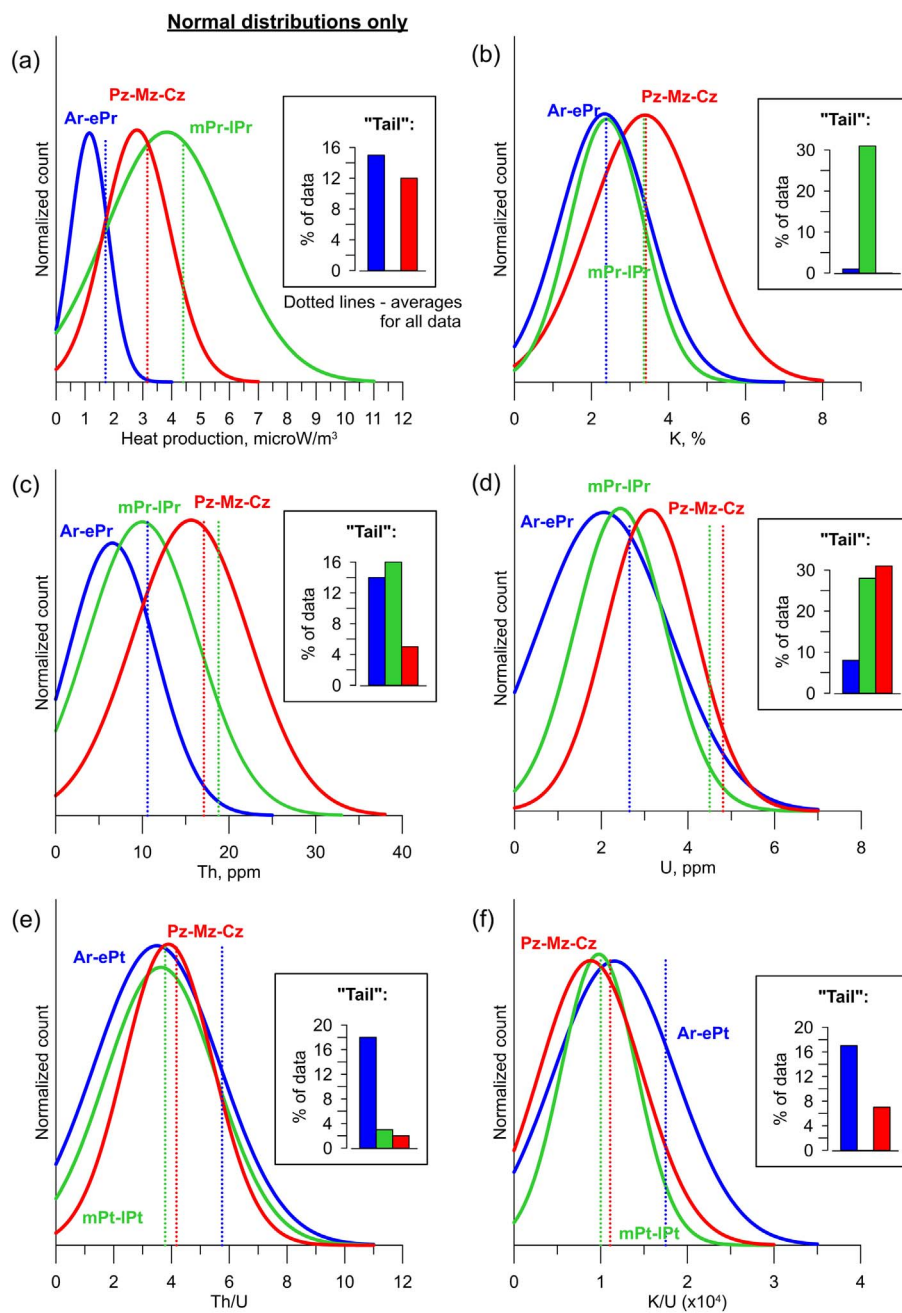


Fig. 27. Summary of statistics for distribution A, concentrations of Th, U, K, and Th/U and K/U ratios in granitic rocks of different ages. All blue lines correspond to Archean – Early Proterozoic rocks, green lines – to Middle and Late Proterozoic rocks, red lines – to Phanerozoic rocks. Bell-shaped lines show normal distributions normalized by the maximum count (for details see Figs. 8, 13–15, 19–20). Dashed vertical lines give the average value calculated for all data (that is data that makes both normal distribution and the “tail” (see Tables 11–12 for details). Small boxes show the percentage of data points that make the “tails”. When all data are included in statistics, average concentrations of Th, U and K in Middle-Late Proterozoic and Phanerozoic rocks are similar. However, if only data that makes normal distributions is considered, old granitic rocks have lower concentrations of radiogenic elements than younger rocks. Note that, statistically, Middle-Late Proterozoic granitic rocks have higher heat production than Phanerozoic rocks (compare with Fig. 7). (For interpretation of the references to color in this figure legend, the reader is referred to the web version of this article.)

granitic magmas and emplacement of granitic rocks with their possible later chemical alteration. The general statistics critically depends on how much data is included into the analysis, i.e. if one includes all data or only data that falls within 1σ of the mean value for a normal distribution (Fig. 27).

The granite subset that follows normal distributions for the abundances of Th, U, and K, have mean values close to the average upper continental crust (compare Tables 1 and 11). When all data, including “the tails”, is used for the analysis, the values of Th and U concentrations are 50–60% higher (compare Tables 1 and 12).

4. Archean-Early Proterozoic granites, including granites of the global-scale 2.1–1.8 Ga collisional event, all have a narrower distribution of heat production than the post-1.8 Ga granites (Figs. 8, 27), and high-value outliers with $A > 2.5 \mu\text{W}/\text{m}^3$ (“the tail” of the normal distribution) are rare. We speculate that processes of granitic

magma generation were more uniform in the early Earth than at later times and were possibly dominated by collisional environments.

In general, Archean-Early Proterozoic granitic rocks have low concentrations of Th, U and K and, as a consequence, low heat production (Fig. 27) ($A = 1.17 \pm 0.67 \mu\text{W}/\text{m}^3$ for the normal distribution data and $1.71 \pm 1.68 \mu\text{W}/\text{m}^3$ for all data). We speculate that low radiogenic heat production in ancient continental crust may play an important role in preservation of cratonic lithosphere in the geological record.

5. Our data does not show a monotonic secular trend in heat production with age of the granites. Instead heat production shows a remarkable peak in Middle Proterozoic granites (presently $A = 3.83 \pm 2.14 \mu\text{W}/\text{m}^3$ for the normal distribution data and $A = 4.40 \pm 2.39 \mu\text{W}/\text{m}^3$ for all data), followed by a gradual

decrease in present heat production since ca. 2 Ga (Figs. 7 and 27). This peak is even more pronounced when back-projected to the granite emplacement age (Fig. 18).

We speculate that the Middle Proterozoic marks a sharp change in geodynamic settings for granitic magma generation which may be caused by major plate reorganizations possibly related to the supercontinent cycle and the assembly of the supercontinent Nuna (Columbia). Middle-Late Proterozoic granites also have a very broad distribution for heat production (Fig. 27). We infer that Middle Proterozoic granitic rocks were formed in diverse geodynamic environments, which range from accretional magmatic belts and subduction zones along continental margins to intracratonic settings with involvement of large volumes of mantle material in production of anorogenic granites by mantle plumes.

Our results also suggest (Fig. 18) that plate tectonics may have been faster in the Archean than in the Early Proterozoic, but the fastest plate motions may have been in the Middle Proterozoic followed by a continuous slowing down since then.

6. Phanerozoic granites have the highest concentrations of Th, U and K and, as a consequence, high heat production (Fig. 27) ($A = 2.79 \pm 1.14 \mu\text{W/m}^3$ for normal distribution and $3.16 \pm 1.74 \mu\text{W/m}^3$ for all data), which gradually decreases from Paleozoic to Cenozoic granites for the present-day values (Fig. 7) but remains nearly constant when recalculated to the time of the granite emplacement (Fig. 18). Similar to Middle-Late Proterozoic granites, Phanerozoic granites have a broad normal distribution (Fig. 8). We speculate that a broad variability of heat production in the Phanerozoic granites reflects the diversity of tectonic environments where they are formed.
7. The present-day Th/U and K/U ratios are close to the expected global values only for the granitic rocks that fall within $\pm 1\sigma$ of the mean for the normal distribution (3.68 ± 1.84 and $0.93 \pm 0.53 [\times 10^4]$, respectively). Global average values based on all data are significantly higher ($\text{Th}/\text{U} = 4.75 \pm 4.27$ and $\text{K}/\text{U} = 1.46 \pm 1.53 [\times 10^4]$).

Anomalously high present-day ratios of Th/U and K/U (“the tail”) all seem to be restricted to Archean – Early Proterozoic granitic rocks (Figs. 19–20). We do not observe a secular monotonous change of Th/U and K/U ratios with the age of granites when all data are included (Table 12). Instead the results show remarkably high ratios in Archean-Early Proterozoic granites ($\text{Th}/\text{U} = 5.75 \pm 5.96$ and $\text{K}/\text{U} = 1.75 \pm 1.84 [\times 10^4]$) with minimum values in Middle-Late Proterozoic granites ($\text{Th}/\text{U} = 3.78 \pm 2.69$ and $\text{K}/\text{U} = 0.99 \pm 0.45 [\times 10^4]$).

The Th/U and K/U ratios recalculated to the time of granite emplacement show a strong variability with an extremely high K/U ratio for the Archean-Early Proterozoic granites (ca. $2.6\text{--}3.9 [\times 10^4]$) and a low Th/U ratio (2.78) for the Archean granites. There seems to be a gradual decrease in both Th/U and K/U ratios from Early Proterozoic until present (Fig. 24).

8. The estimates of the total present-day heat production yield a value of $5.8\text{--}6.8 \text{ TW}$ in the granitic crust and $7.8\text{--}8.8 \text{ TW}$ in the continental crust, assuming that granitic rocks make $1/3$ of its volume. In this case, the global total surface heat flow may be as high as $47\text{--}48 \text{ TW}$.

Supplementary data to this article can be found online at <http://dx.doi.org/10.1016/j.earscirev.2017.07.003>.

Acknowledgments

The idea of the granite data compilation paper came from

discussions between IA and Nelson Eby during a field trip in Turkey in 2014. The global database of heat production in granites (GRANITE2017) was compiled as a part of BS theses of KJ, NKS and LSKN (IGN, University of Copenhagen, 2015). The database is freely available for download as electronic attachment. KJ, LSKN and NKS thank Haibin Yang for providing data for China. The authors are grateful to N. Arndt and an anonymous reviewer whose constructive comments led to a significant extension of the discussion part. Research grant DFF-1323-00053 (Denmark) to IMA is gratefully acknowledged.

Statement on authors' contributions: KJ, LSKN and NKS have compiled the database GRANITE2017 and made its preliminary analysis. IA has developed the idea of the study, made the analysis, wrote most of the text, and prepared figures. HT contributed to the project work and to the text. All authors took part in discussions of the results.

References

- Abbott, D., Burgess, L., Longhi, J., Smith, W., 1994. An empirical thermal history of the Earth's upper mantle. *J. Geophys. Res.* 99 (B7), 13835–13850.
- Albarède, F., 1998. Time-dependent models of U-Th-He and K-Ar evolution and the layering of mantle convection. *Chem. Geol.* 145, 413–429.
- Allegre, C., Manhes, G., Lewin, E., 2001. Chemical composition of the Earth and the volatility control on planetary genetics. *Earth Planet. Sci. Lett.* 185, 49–69.
- Amelin, Y., Lee, D.C., Halliday, A.N., Pidgeon, R.T., 1999. Nature of the Earth's earliest crust from hafnium isotopes in single detrital zircons. *Nature* 399, 252–255.
- Araki, T., et al., 2005. Experimental investigation of geologically produced antineutrinos with KamLAND. *Nature* 436, 499–503.
- Arevalo Jr., R., McDonough, W.F., Luong, M., 2009. The K/U ratio of the silicate Earth: insights into mantle composition, structure and thermal evolution. *Earth Planet. Sci. Lett.* 278, 361–369.
- Arevalo, R., et al., 2013. Simplified mantle architecture and distribution of radiogenic power. *Geochem. Geophys. Geosyst.* 14, 2265–2285.
- Armstrong, R.L., 1981. Radiogenic isotopes: the case for crustal recycling on a near steady-state no-continental growth. *Earth. Phil. Trans. R. Soc. London Ser. A* 301, 443–472.
- Artemieva, I.M., 2006. Global $1^\circ \times 1^\circ$ thermal model TC1 for the continental lithosphere: implications for lithosphere secular evolution. *Tectonophysics* 416, 245–277.
- Artemieva, I.M., 2011. The Lithosphere: An Interdisciplinary Approach. Cambridge University Press <http://dx.doi.org/10.1017/CBO9780511975417>. (794 pp.).
- Artemieva, I.M., Mooney, W.D., 2001. Thermal structure and evolution of Precambrian lithosphere: a global study. *J. Geophys. Res.* 106, 16387–16414.
- Artemieva, I.M., Thybo, H., 2013. EUNASEi: a seismic model for Moho and crustal structure in Europe, Greenland, and the North Atlantic region. *Tectonophysics* 609, 97–153.
- Ashwal, L.D., Morgan, P., Kelley, S.A., Percival, J.A., 1987. Heat production in an Archean crustal profile and implications for heat flow and mobilization of heat-producing elements. *Earth Planet. Sci. Lett.* 85, 439–450.
- Beardsmore, G.R., Cull, J.P., 2001. Crustal Heat Flow. Cambridge University Press, A Guide to Measurement and Modeling.
- Belousova, E.A., Kostitsyn, Y.A., Griffin, W.L., Begg, G.C., O'Reilly, S.Y., Pearson, N.J., 2010. The growth of the continental crust: constraints from zircon Hf-isotope data. *Lithos* 119, 457–466.
- Birch, F., 1954. Heat from radioactivity. In: Faul, H. (Ed.), Nuclear Geology. John Wiley and Sons, New York, N.Y., pp. 148–174.
- Bonin, B., 2007. A-type granites and related rocks: evolution of a concept, problems and prospects. *Lithos* 97, 1–29.
- Buntebarth, G., 1976. Distribution of uranium in intrusive bodies due to combined migration and diffusion. *Earth Planet. Sci. Lett.* 32, 84–90.
- Chappell, B.W., White, A.J.R., 1974. Two contrasting granite types. *Pac. Geol.* 8, 173–174.
- Chappell, B.W., White, A.J.R., 1992. I- and S-type granites in the Lachlan Fold Belt. *Trans. R. Soc. Edinb. Earth Sci.* 83, 1–26.
- Chappell, B.W., White, A.J.R., 2001. Two contrasting granite types – 25 years later. *Aust. J. Earth Sci.* 48, 489–499.
- Cherepanova, Y., Artemieva, I.M., Thybo, H., Chemia, Z., 2013. Crustal structure of the Siberian Craton and the West Siberian Basin: an appraisal of existing seismic data. *Tectonophysics* 609, 154–183.
- Christensen, N.I., Mooney, W.D., 1995. Seismic velocity structure and composition of the continental-crust – a global view. *J. Geophys. Res.* 100, 9761–9788.
- Clemens, J.D., Wall, V.J., 1981. Origin and crystallization of some peraluminous (S-type) granitic magmas. *Can. Mineral.* 19, 111–131.
- Collins, W.J., Beams, S.D., White, A.J.R., Chappell, B.W., 1982. Nature and origin of A-type granites with particular reference to southeastern Australia. *Contrib. Mineral. Petrol.* 80, 189–200.
- Condie, K.C., 1993. Chemical composition and evolution of the upper continental crust: contrasting results from surface samples and shales. *Chem. Geol.* 104, 1–37.
- Condie, K.C., 1998. Episodic continental growth and supercontinents: a mantle avalanche connection? *Earth Planet. Sci. Lett.* 163, 97–108.
- Condie, K.C., 2014. Growth of continental crust: a balance between preservation and recycling. *Mineral. Mag.* 78 (3), 623–637.
- Davies, G.F., 1999. Geophysically constrained mantle mass flows and the 40Ar budget: a

- degassed lower mantle? *Earth Planet. Sci. Lett.* 166, 149–162.
- Deschamps, F., Tackley, P.J., Nakagawa, T., 2010. Temperature and heat flux scalings for isoviscous thermal convection in spherical geometry. *Geophys. J. Int.* 182, 137–154.
- Eby, N.G., 1992. Chemical subdivision of the A-type granitoids: petrogenetic and tectonic implications. *Geology* 20, 641–644.
- Eby, G.N., 2011. A-type granites: magma sources and their contribution to the growth of the continental crust. In: Seventh Hutton Symposium on Granites and Related Rocks, pp. 50–51.
- Eder, G., 1966. Terrestrial neutrinos. *Nucl. Phys.* 78, 657–662.
- Fountain, D.M., 1985. Is there a relationship between seismic velocity and heat production for crustal rocks? *Earth Planet. Sci. Lett.* 79, 145–150.
- Fountain, D.M., 1986. Is there a relationship between seismic velocity and heat production for crustal rocks? *Earth Planet. Sci. Lett.* 79, 145–150.
- Fountain, D.M., Salisbury, M.H., Furlong, K.P., 1987. Heat production and thermal conductivity of rocks from the Pikwitonei-Sachigo continental cross-section, central Manitoba: implications for the thermal structure of Archean crust. *Can. J. Earth Sci.* 24, 1583–1594.
- Frost, B.R., Barnes, C., Collins, W.J., Arculus, R.J., Ellis, D., Frost, C.D., 2001. A geochemical classification for granitic rocks. *J. Petrol.* 42, 2033–2044.
- Furukawa, Y., Shinjoe, H., 1997. Distribution of radiogenic heat generation in the arc's crust of the Hokkaido island, Japan. *Geophys. Res. Lett.* 24, 1279–1282.
- Gao, S., Luo, T.-C., Zhang, B.-R., Zhang, H.-F., Han, Y.-W., Hu, Y.-K., Zhao, Z.-D., 1998. Chemical composition of the continental crust as revealed by studies in East China. *Geochim. Cosmochim. Acta* 62, 1959–1975.
- Guillouf-Frottier, L., Mareschal, J.-C., Jaupart, C., Gariepy, C., Lapointe, R., Bienfait, G., 1995. Heat flow variations in the Grenville Province, Canada. *Earth Planet. Sci. Lett.* 136, 447–460.
- Hacker, B.R., Kelemen, P.B., Behn, M.D., 2011. Differentiation of the continental crust by relamination. *Earth Planet. Sci. Lett.* 307 (3–4), 501–516. <http://dx.doi.org/10.1016/j.epsl.2011.05.024>.
- Hamilton, W.B., 2013. Evolution of the Archean Mohorovičić discontinuity from a synaccretionary 4.5 Ga protocrust. In: H. Thybo, I. Artemieva and B. Kennett (Eds.), "Moho: 100 years after Andrija Mohorovičić". *Tectonophysics* 609, 706–734.
- Harrison, T.M., Blighert-Toft, J., Muller, W., Albareda, F., Holden, P., Mojzsis, S.J., 2005. Heterogeneous Hadean hafnium: evidence of continental crust at 4.4 to 4.5 Ga. *Science* 310, 1947–1950.
- Hawkesworth, C.J., Kemp, A.I.S., 2006. Evolution of the continental crust. *Nature* 443, 811–817.
- Hawkesworth, C., Cawood, P., Kemp, A., Storey, C., Dhuime, B., 2009. A matter of preservation. *Science* 323, 49–50.
- Huang, Y., Chubakov, V., Mantovani, F., Rudnick, R.L., McDonough, W.F., 2013. A reference Earth model for the heat producing elements and associated flux. *Geochim. Geophys. Geosyst.* 14, 2003–2029. <http://dx.doi.org/10.1002/ggge.20129>.
- Inger, S., Harris, N., 1993. Geochemical constraints on leucogranite magmatism in the Langtang valley, Nepal Himalaya. *J. Petrol.* 34, 345–368.
- Jaupart, C., Mareschal, J.-C., 2003. Constraints on crustal heat production from heat flow data. In: Rudnick, R.L. (Ed.), *The Crust, Vol. 3 Treatise on Geochemistry* (Eds. H.D. Holland and K.K. Turekian). Elsevier-Pergamon, Oxford, pp. 65–84.
- Jaupart, C., Labrosse, S., Mareschal, J.-C., 2007. Temperatures, heat and energy in the mantle of the Earth. In: Schubert, G. (Ed.), *Treatise on Geophysics*. vol. 1 Elsevier, New York.
- Jochum, K.P., Hofmann, A.W., Ito, E., Seufert, H.M., White, W.M., 1983. K, U and Th in mid-ocean ridge basalt glasses and heat production, K/U and K/Rb in the mantle. *Nature* 306, 431–436.
- Jones, M.Q.W., 1987. Heat flow and heat production in the Namaqua mobile belt, South Africa. *J. Geophys. Res.* 92, 6273–6289.
- Kelemen, P.B., 1995. Genesis of high Mg# andesites and the continental crust. *Contrib. Mineral. Petrol.* 120, 1–19.
- Kemp, A.I.S., 2001. The Petrogenesis of Granitic Rocks: A Source-based Perspective. (PhD Thesis) The Australian National University, Canberra.
- Kemp, A.I.S., Hawkesworth, C.J., 2003. Granitic perspectives on the generation and secular evolution of the continental crust. In: Rudnick, R.L. (Ed.), *The Crust, Vol. 3, Treatise on Geochemistry* (Eds. H.D. Holland and K.K. Turekian). Elsevier-Pergamon, Oxford, pp. 349–410.
- Ketcham, R.A., 1996. Distribution of heat-producing elements in the upper and middle crust of southern and west central Arizona: evidence from the core complexes. *J. Geophys. Res.* 101, 13611–13632.
- Kobayashi, M., Fukao, Y., 1991. The Earth as antineutrino star. *Geophys. Res. Lett.* 18, 633–636.
- Korenaga, J., 2006. Archean geodynamics and the thermal evolution of Earth. In: Benn, K., Mareschal, J.-C., Condie, K. (Eds.), *Archean Geodynamics and Environments*. AGU, Washington, D. C, pp. 7–32.
- Korenaga, J., 2008. Urey ratio and the structure and evolution of Earth's mantle. *Rev. Geophys.* 46, RG2007.
- Krauss, L., Glashow, S.L., Schramm, D.N., 1984. Antineutrino astronomy and geophysics. *Nature* 310, 191–198.
- Kukkonen, I.T., Lahtinen, R., 2001. Variation of radiogenic heat production rate in 2.8–1.8 Ga old rocks in the central Fennoscandian Shield. *Phys. Earth Planet. Inter.* 126, 2279–2294.
- Kukkonen, I.T., Peltoniemi, S., 1998. Relationships between thermal and other petrophysical properties of rocks in Finland. *Phys. Chem. Earth* 23, 341–349.
- Lassiter, J.C., 2004. Role of recycled oceanic crust in the potassium and argon budget of the Earth: toward a resolution of the “missing argon” problem. *Geochem. Geophys. Geosyst.* 5. <http://dx.doi.org/10.1029/2004GC000711>.
- Loiselle, M.C., Wones, D.R., 1979. Characteristics and origin of anorogenic granites. In: *Geol. Soc. America, Abstracts With Programs* 11, No. 7. 468.
- Lyubetskaya, T., Korenaga, J., 2007. Chemical composition of Earth's primitive mantle and its variance: 1. Method and results. *J. Geophys. Res.* 112 (B3), B03211.
- Mantovani, F., Carmignani, L., Fiorentini, G., Lissia, M., 2004. Antineutrinos from Earth: a reference model and its uncertainties. *Phys. Rev. D* 69, 013001.
- Martin, H., 1995. Archean grey gneisses and the genesis of continental crust. In: Condie, K.C. (Ed.), *Archean Crustal Evolution*. Elsevier, Netherlands, pp. 205–260.
- McDonough, W.F., 2005. Ghosts from within. *Nature* 436, 467–468.
- McDonough, W.F., Sun, S.-S., 1995. The composition of the Earth. *Chem. Geol.* 120, 223–253.
- McLennan, S.M., 2001. Relationships between the trace element composition of sedimentary rocks and upper continental crust. *Geochem. Geophys. Geosyst.* 2 (4). <http://dx.doi.org/10.1029/2000gc000109>.
- McLennan, S.M., Taylor, S.R., 1996. Heat flow and the chemical composition of continental crust. *J. Geol.* 104, 377–396.
- Nakagawa, T., Tackley, P., 2012. Influence of magmatism on mantle cooling, surface heat flow and Urey ratio. *Earth Planet. Sci. Lett.* 329–330, 1–10.
- Nicolaysen, L.O., Hart, R.J., Gale, N.H., 1981. The Vredefort radioelement profile extended to supracrustal strata at Carletonville, with implications for continental heat flow. *J. Geophys. Res.* 86, 10653–10661.
- Pinet, C., Jaupart, C., 1987. The vertical distribution of radiogenic heat production in the Precambrian crust of Norway and Sweden: geothermal implications. *Geophys. Res. Lett.* 14, 260–263.
- Pollack, H.N., Hurter, S.J., Johnston, J.R., 1993. Heat loss from the Earth's interior: analysis of the global data set. *Rev. Geophys.* 31, 267–280.
- Reimink, J.R., Davies, J.H.F.L., Chacko, T., Stern, R.A., Heaman, L.M., Sarkar, C., Schaltegger, U., Creaser, R.A., Pearson, D.G., 2016. No evidence for Hadean continental crust within Earth's oldest evolved rock unit. *Nat. Geosci.* 9, 777–780.
- Rogers, J.J., Santosh, M., 2002. Configuration of Columbia, a Mesoproterozoic supercontinent. *Gondwana Res.* 5 (1), 5–22.
- Roy, S., Rao, R.U.M., 2000. Heat flow in the Indian shield. *J. Geophys. Res.* 105, 25587–25604.
- Rudnick, R.L., 1995. Making continental crust. *Nature* 378, 573–578.
- Rudnick, R.L., Fountain, D.M., 1995. Nature and composition of the continental crust: a lower crustal perspective. *Rev. Geophys.* 33, 267–309.
- Rudnick, R.L., Gao, S., 2003. Composition of the continental crust. In: Rudnick, R.L. (Ed.), *The Crust, Vol. 3, Treatise on Geochemistry* (Eds. H.D. Holland and K.K. Turekian). Elsevier-Pergamon, Oxford, pp. 1–64.
- Rudnick, R.L., Nyblade, A.A., 1999. The thickness and heat production of Archean lithosphere: constraints from xenolith thermobarometry and surface heat flow. In: Fei, Y., Bertka, C.M., Mysen, B.O. (Eds.), *Mantle Petrology: Field Observations and High Pressure Experimentation: A Tribute to Francis R. (Joe) Boyd*. Chem. Soc. Spec. Publ. No. 6, pp. 3–12.
- Rudnick, R.L., Presper, T., 1990. Geochemistry of intermediate to high-pressure granulites. In: Vielzeuf, D., Vidal, P. (Eds.), *Granulites and Crustal Evolution*. Kluwer, Netherlands, pp. 523–550.
- Rudnick, R.L., McDonough, W., O'Connell, R.J., 1998. Thermal structure, thickness and composition of continental lithosphere. *Chem. Geol.* 145, 395–411.
- Rybachi, L., 1988. Determination of heat production rate. In: Haenel, R., Rybachi, L., Stegema, L. (Eds.), *Handbook of Terrestrial Heat-flow Density Determination*. Kluwer Academic Press, pp. 125–142.
- Rybachi, L., Buntebarth, G., 1982. Relationship between the petrophysical properties density, seismic velocity, heat generation and mineralogical constitution. *Earth Planet. Sci. Lett.* 57, 367–376.
- Salters, V.J.M., Stracke, A., 2004. Composition of the depleted mantle. *Geochem. Geophys. Geosyst.* 5, Q05B07. <http://dx.doi.org/10.1029/2003GC000597>.
- Shaw, D.M., Cramer, J.J., Higgins, M.D., Truscott, M.G., 1986. Composition of the Canadian Precambrian shield and the continental crust of the Earth. In: Dawson, J.B., Carswell, D.A., Hall, J., Wedepohl, K.H. (Eds.), *Nature of the Lower Continental Crust*, Geological Society of London (UK) Special Pub. 24. pp. 275–282.
- Sylvester, P.J., 1995. Archean granite plutons. In: Condie, K.C. (Ed.), *Archean Crustal Evolution*. Elsevier, Netherlands, pp. 261–314.
- Taylor, S.R., McLennan, S.M., 1985. *The Continental Crust: Its Composition and Evolution*. (312 pp.) Blackwell, Oxford.
- Taylor, S.R., McLennan, S.M., 1995. The geochemical evolution of the continental crust. *Rev. Geophys.* 33, 241–265.
- The KamLand Collaboration, 2011. Partial radiogenic heat model for Earth revealed by geoneutrino measurements. *Nat. Geosci.* 4, 647–651.
- Usman, S.M., et al., 2015. AGM2015: antineutrino global map 2015. *Sci Rep* 5, 13945.
- Van Schmus, W.R., 1995. Natural radioactivity of the crust and mantle. In: *Global Earth Physics: A Handbook of Physical Constants* (AGU Reference Shelf 1).
- Vila, M., Fernández, M., Jiménez-Munt, I., 2010. Radiogenic heat production variability of some common lithological groups and its significance to lithospheric thermal modeling. *Tectonophysics* 490, 152–164.
- Weaver, B.L., Tarney, J., 1984. Empirical approach to estimating the composition of the continental crust. *Nature* 310, 575–577.
- Wedepohl, K.H., 1995. The composition of the continental crust. *Geochim. Cosmochim. Acta* 59 (7), 1217–1232. [http://dx.doi.org/10.1016/0016-7037\(95\)00038-2](http://dx.doi.org/10.1016/0016-7037(95)00038-2).
- Whalen, J.B., 1985. Geochemistry of an island-arc plutonic suite: the Uasila-Yau Yau intrusive complex, New Britain PNG. *J. Petrol.* 26, 603–632.
- White, A.J.R., 1979. Sources of granite magmas. *Geol. Soc. Am. Abstr. Programs* 11 (7), 539.
- Wollenberg, H.A., Smith, A.R., 1987. Radiogenic heat production of crustal rocks: an assessment based on geochemical data. *Geophys. Res. Lett.* 14, 295–298.
- Wormald, R.J., Price, R.C., 1988. Peralkaline granites near Temora, southern New South Wales: tectonic and petrological implications. *Aust. J. Earth Sci.* 35, 209–221.
- Xia, B., Thybo, H., Artemieva, I.M., 2017. Seismic crustal structure of the North China

Craton and surrounding area: synthesis and analysis. *J. Geophys. Res.* <http://dx.doi.org/10.1002/2016JB013848>.

Zhao, G., Cawood, P.A., Wilde, S.A., Sun, M., 2002. Review of global 2.1–1.8 Ga orogens:

implications for a pre-Rodinia supercontinent. *Earth Sci. Rev.* 59 (1), 125–162.

Zhao, G., Sun, M., Wilde, S.A., Li, S., 2004. A Paleo-Mesoproterozoic supercontinent: assembly, growth and breakup. *Earth Sci. Rev.* 67 (1), 91–123.